Predictive Crypto Crashes and Asset Pricing Implications: An Inelastic Market Perspective

Jennifer (Jie) Li[*] **Li Liao**[†] **Siyuan Yang**[‡] **Hong Zhang**[§]

This Draft: June 2025

Abstract

Frequent and large-scale crashes are hallmarks of cryptocurrencies. We propose a new mechanism to explain this phenomenon: blockchain-based capital inelasticity. Empirically, inelastic cryptocurrencies underperform elastic ones, reflecting inelasticity-induced crash risk. This effect persists even among past winners, suggesting that crash risk dominates momentum among inelastic cryptocurrencies. Consequently, only elastic cryptocurrencies deliver significant momentum returns, allowing a strategy that combines inelastic crashes and elastic momentum to generate higher returns with longer durations than momentum. Analysis of ICO-induced Ethereum blockchain congestion supports a causal interpretation of our mechanism. Our results highlight the importance of inelastic capital in shaping cryptocurrency prices.

JEL classification codes: G10 G12 G14 O30

Keywords: Blockchain, Cryptocurrency, Slow-moving capital, Crashes, Momentum, FinTech, Inelastic Market

[*] Business Administration University of Macau, E22 Avenida da Universidade, Taipa, Macau, China; E-mail: jenniferli@um.edu.mo.

† PBCSF, Tsinghua University, 43 Chengfu Road, Beijing, PR China, 100083, E-mail: liaol@pbcsf.tsinghua.edu.cn.

‡ China School of Banking and Finance, University of Internation Business and Economics, 100029; Email: yangsy@uibe.edu.cn.

§ Singapore Management University, 50 Stamford Road #4087, Singapore 178899; Email: hongzhang@smu.edu.sg.

I. Introduction

Blockchain lies at the heart of the Fintech revolution and is widely regarded as a disruptive force across a broad range of industries. Since the launch of Bitcoin, the first blockchain-based cryptocurrency, in 2009, thousands of cryptocurrencies have emerged, built on similar or enhanced blockchain platforms. While cryptocurrencies (or cryptos for simplicity) possess numerous novel attributes and have recently attracted the interest of the U.S. government, what garners the most public attention is the occurrence of bubbles and crashes with unprecedented scale and intensity. For instance, Bloomberg reported an 80% market-wide plunge during the "Great Crypto Crash" of early 2018, a collapse that dwarfed even the infamous Dot-Com crash.[1] These extreme events urge researchers to delve into the asset pricing foundation of blockchain-based assets.

We propose that crypto crashes may be deeply rooted in a key limitation of blockchain technologies: scalability and capacity constraints in processing transactions. Blockchain underpins decentralized digital ledgers through peer-to-peer networks, public-key cryptography, and consensus mechanisms, making transactions and data validation inherently costly. As a result, Abadi and Brunnermeier (2022) propose a "blockchain trilemma" where consensus mechanisms cannot simultaneously achieve fault tolerance, resource efficiency, and full transferability. Similarly, Cong and He (2019) identify a fundamental tension between decentralized consensus and information dissemination. Hinzen, John, and Saleh (2022) show that blockchain delay may give rise to negative network effects. From a capital flow perspective, these properties limit the speed and scale at which capital can move across the market to join transactions, naturally giving rise to *slow-moving* or *inelastic* capital (we will use these two terminologies interchangeably).[2]

To understand how slow-moving capital can give rise to crypto crashes, consider a scenario where crypto investors encounter blockchain congestion.[3] During such periods, more capital remains on the sidelines, waiting to be executed rather than actively participating in trades. In this case, capital becomes "slower" or more "inelastic" in absorbing potential shocks (Duffie 2010 provides more examples of slow-moving capital). Investors face increased trading frictions,

---

[1] https://www.bloomberg.com/news/articles/2018-09-12/crypto-s-crash-just-surpassed-dot-com-levels-as-losses-reach-80.

[2] For instance, the flows of capital across exchanges and wallets on the public blockchains are slow, allowing within-exchange shocks to create cross-exchange arbitrate opportunities (e.g., Makarov and Schoar, 2019).

[3] Of course, blockchain congestion is not the only mechanism of slow-moving capital in the crypto market. However, this connection provides an intuitive economic ground for us to develop hypotheses and design identification tests. The existence of other mechanisms will not contaminate the main concolusions of our analysis on slow-moving capital.

encompassing not only trading inconveniences like execution delays but also heightened risks due to large price swings. These price swings arise because, in theory (Duffie, Gârleanu, and Pedersen 2005, 2007; Duffie 2010), a leading feature of slow-moving capital is the occurrence of sharp price shifts followed by reversals. The initial price shift occurs when the small subset of immediately available capital fails to absorb shocks, and the price reverses when more capital becomes available.

Our new intuition is that experiencing the inconveniences and risks of capital inelasticity may compel at least some investors to reduce their demand. Since reduced demand occurs when inelasticity is high, the resulting price decline could be significantly more severe than what a comparable demand shift would generate with elastic capital. This "magnified" price drop arises naturally from the previously mentioned theories of slow-moving capital and also aligns with the price impact of demand shocks in inelastic markets (Koijen and Yogo, 2019; Gabaix and Koijen, 2021). We refer to such price declines as *inelastic crypto crashes* because of their relative severity. A testable implication is that capital inelasticity may predict inelastic crashes, as such inelasticity is likely to trigger inward demand shifts and cause prices to collapse.

In addition to being predictive, inelastic crashes exhibit another intriguing property: they contradict one of the most well-documented anomalies in finance—momentum. Under momentum, a crypto with a high recent return generally generates high future returns (Liu and Tsyvinski, 2021; Liu, Tsyvinski, and Wu, 2022; Cong, Karolyi, Tang, and Zhao, 2023). However, if the high return originates from inelastic capital—whether due to an initial price drift caused by unmatched excess demand or a reversal from a prior substantial price drawdown—the heightened risk of subsequent inelastic crashes could offset the continuation of positive returns. In other words, among momentum winners, only those produced by elastic cryptos (i.e., elastic winners) are expected to sustain returns. In contrast, inelastic winners will likely underperform elastic winners due to crash risk. The difference between elastic and inelastic losers is less pronounced, as both momentum and crash predict a continuation of negative returns. Nonetheless, the underperformance of inelastic losers could be more enduring as the two effects reinforce each other.

The above discussion suggests a novel set of asset pricing implications. First, momentum may perform well among elastic cryptos (i.e., *elastic momentum*) but not in inelastic ones. Moreover, a portfolio strategy that combines elastic momentum with inelastic crashes—i.e., buying elastic winners and selling inelastic losers—will likely generate higher and more persistent returns. This *ElasticWinner-minus-InelasticLoser* (EWIL) strategy can outperform traditional momentum by excluding inelastic winners and focusing on inelastic losers. Lastly, since it may take longer for the market with inelastic capital to reach equilibrium, EWIL is also expected to deliver higher returns over a more extended holding period than traditional momentum.

We test the above predictions based on a sample of 4284 cryptocurrencies from 2014 to May 2024. One empirical challenge is the lack of direct measures on capital inelasticity and underlying blockchain congestion. Most cryptos do not even have reported blockchain information. To address this issue, we adopt an indirect "revealed preference" approach: we use the leading outcome of slow-moving capital—i.e., substantial price movements followed by a reversal—to infer the degree of capital inelasticity. More specifically, we calculate the maximum price runup (*MaxRunup*) and price drawdown (*MaxDrawdown*) experienced by a cryptocurrency during a quarterly ranking period. Since the two opposite price movements cannot occur simultaneously, a high rank in both events indicates the sequential occurrence of large price movements with opposite signs—consistent with a jump-reversal pattern. Consequently, we can use the average rank of *MaxRunup* and *MaxDrawdown* to quantify the severity of jump-reversal events, serving as our main proxy for the degree of capital inelasticity (hereafter referred to as *Inelastic Rank* or *InRank*).

To set the stage, we first introduce two diagnostic tests to illuminate the economic insights of our measure. The first test uses the subsample of cryptos with blockchain information to construct two blockchain-based proxies for slow-moving capital: the average time between transactions (*Time*) and its interaction with the number of transactions (*Time*×*Volume*). The first variable is a widely recognized measure of blockchain congestion; a longer *Time* reduces the speed at which capital can participate in trades, thereby reflecting slower-moving capital. Moreover, during periods of congestion, increased trading demand often causes more capital to remain stuck for longer durations while competing for limited blockchain resources. As a result, the interaction between *Time* and *Volume* amplifies capital inelasticity.[4] Empirically, we observe that *InRank* is positively related to both indicators, suggesting that our measure reasonably captures the concept of slow-moving capital on the blockchain.

The second diagnostic test examines the relationship between crypto returns and the two components of *InRank*—*MaxRunup* and Max*Drawdown*. At the beginning of each weekly holding period, we independently sort crypto into three groups (30%-40%-30%) based on each component

[4] This effect is consistent with the theoretical prediction that constraints on transaction rates and increased transaction demand will lead to substantial price responses (e.g., Hinzen, John, and Saleh, 2022). This effect is often aggravated by infrastructure failure.

observed during the preceding quarterly rank period. The portfolios are then rebalanced weekly. Interestingly, high *MaxRunup* ranks do not lead to high returns, contrary to what momentum would suggest. Instead, risk-adjusted value-weighted holding-period returns decline in both ranks, leading to a trough in the top/top portfolio. When we use the mid/mid portfolio as a benchmark, the top/top portfolio underperforms with a return spread of -2.6% per week. The spread narrows slightly to -2.3% when risk-adjusted by Liu, Tsyvinski, and Wu's (2022) three-factor and -2.1% when adjusted by Cong, Karolyi, Tang, and Zhao's (2023) five-factor models.

Collectively, our diagnostic tests suggest that *InRank* aligns closely with indicators of inelastic capital and that its two components are strong predictors for crashes. Hence, while the measure is indirect, it provides a reasonable metric for testing the asset pricing implications of inelastic capital. Any remaining noise works only against us in finding significant results.

Equipped with this measure, we formally investigate the asset pricing implications of inelastic capital. We start with two analyses of inelastic crashes. In the first portfolio analysis, we sort cryptocurrencies into five quintiles according to their *InRank* observed during the quarterly ranking period and rebalance these portfolios weekly. Cryptos in the most inelastic quintile exhibit a significantly higher crash risk than those in the most elastic quintile. An Elastic-minus-Inelastic (EMI) strategy, which buys (short-sells) the value-weighted portfolio of cryptos in the most elastic (inelastic) quintile, can generate a significant out-of-sample weekly return of 2.5%. This return spread becomes 2.6% and 2.4% when adjusted by the three- and five-factor models and remains highly significant when we extend holding periods to four or eight weeks.

Our second multivariate regression analysis further examines the out-of-sample return predictive power of *InRank* when controlling for a list of crypto characteristics, including size, momentum, idiosyncratic volatility, lottery payoffs, Amihud illiquidity, and turnover. We observe that higher *InRank* predicts significantly negative out-of-sample returns in the following week. A one-standard increase in *InRank* is associated with a 1.59% lower out-of-sample weekly returns.[5] This return predictive power also remains highly robust when we use a dummy indicator of top-20% *InRank*, extend the holding period to 4 or 8 weeks, or replace crypto returns with dummy indicators for the occurrence of "crashes" following the definition of Greenwood, Shleifer, and You (2018)—i.e., when crypto returns falling within the bottom 20% in the cross-section.

[5] The standard deviation of *InRank* is 0.2887. Since the regression coefficient is 0.055 (or 5.5%), we calculate the one-standard-deviation predictive power of *InRank* as $0.2887 \times 5.5\% = 1.59\%$.

Taken together, the portfolio and multivariate analyses confirm the notion of inelastic crashes. Figure 1 further illustrates the long-term performance of inelastic crash risk by plotting the cumulative returns of value-weighted portfolios with high, mid, and low crypto *InRanks* in the cross-section (using quintile splits, where "mid" includes quintiles 2 to 4). Throughout our sample period, the high-*InRank* portfolio generates persistently negative returns, allowing an Elastic-minus-Inelastic (EMI) strategy to deliver highly positive returns.

We next examine the impact of inelastic crashes on momentum. We first double-sort cryptocurrencies based on past two-week returns and past-quarter *InRank* (using 30%-40%-30% splits). The value-weighted winner-minus-loser (WML) strategy can generate a significant weekly return of 1.3% among all cryptos and 2.1% among the most elastic ones.[6] In contrast, WML fails to deliver positive returns among the most inelastic cryptos. But why? Using elastic WML as a benchmark, we find that the main reason lies in the underperformance of inelastic winners: inelastic winners underperform elastic winners by a significant weekly return of 2.7%, which is comparable to the economic magnitude of elastic momentum. Although inelastic losers also tend to deliver lower returns than elastic losers, their return difference is not as pronounced. Consequently, inelastic winners fail to outperform inelastic losers.

We then investigate the EWIL strategy, which leverages the positive returns generated by elastic winners and the negative returns associated with inelastic losers. We observe that EWIL can generate a highly significant weekly return of 3.4%, which more than doubles the return of momentum (1.4%) or EMI (1.3%). Risk adjustment has little impact on this return spread—the EWIL return remains at 3.3% and 3.2% when adjusted by the three- and five-factor models.

Moreover, EWIL delivers positive returns over a much longer holding horizon than momentum. Crypto momentum typically peaks at a 9-week holding period and then dissipates—its returns eventually turn negative when the holding period exceeds 20 weeks.[7] In contrast, EWIL returns remain robust and do not dissipate even with a holding period of 52 weeks.

Momentum strategies are known to face crash risks (Daniel and Moskowitz 2016). Can EWIL help mitigate this risk? In the stock market, momentum crashes occur because, during bear markets, momentum functions like written call options on the market, leading to substantial losses

[6] We use the weekly holding period immediately after the ranking period because, as indicated by Liu and Tsyvinski (2021), we do not observe a short-term reversal in the cryptocurrency market. Momentum is also observed among cryptos with mid-*InRanks*.

[7] For longer holding horizons, we follow Jegadeesh and Titman (1993) to invest equally in overlapped portfolios of a particular strategy, which allows us to calculate the weekly return of the strategy.

when the market rebounds (Daniel and Moskowitz 2016). This mechanism resembles negative market timing. Although crypto momentum shows insignificant (and still negative) optionality, its market exposure increases significantly during the bear market. As a result, crypto momentum still exhibits significant crash risk. In contrast, EWML demonstrates negligible market exposure and displays positive market timing during bear markets, indicating that shorting inelastic losers enables EWML to hedge against or even capitalize on the risk of market crashes.

Taken together, the above results strongly suggest that capital inelasticity provides a novel economic basis for the risks associated with crypto momentum. Kogan et al., (2024) report that crypto retail investors adopt momentum-like strategies when they expect positive returns to increase future adoption, consistent with the positive network feedback effects modeled by Cong et al., (2021) and Sockin and Xiong (2023a). Our results suggest that capital (in)elasticity may play a crucial role in supporting (or offsetting) this mechanism. While the positive feedback effect plays well among elastic winners, a negative feedback effect may occur when capital becomes inelastic: the inconvenience and risk of inelastic capital, once established (e.g., due to blockchain shocks, which we will discuss shortly), may prompt some investors to withdraw their demand, thereby increasing the inconvenience and risk for remaining investors. Consequently, a "hysteresis" effect may be triggered to amplify price inefficiency in the spirit of Dow, Han, and Sangiorgi (2021), leading to prolonged inelastic crashes. Capital inelasticity, in this regard, introduces a novel source of risk for buy-side momentum.

Thus far, our empirical results support the notion of inelastic crash and its impact on momentum. Given its pivotal role in our analysis, we next provide an identification test on its mechanism using the 50 largest Initial Coin Offerings (ICOs) conducted on the Ethereum blockchain. These ICOs occupy a large portion of the blockchain capacity, crowding out resources available to other cryptos using the same blockchain (i.e., treated cryptos).[8] Consequently, these ICOs create a plausibly exogenous shock of blockchain congestion for treated cryptos.

We accordingly utilize a diff-in-diff (DiD) framework to identify the impact of blockchain congestion. We also use characteristics-matched non-Ethereum blockchain cryptos as the control group (based on Mahalanobis distance) and impose a highly restrictive set of fixed effects. In particular, we use crypto-by-event fixed effects to account for the time-invariant crypto exposure to ICOs and event-by-time fixed effects to capture the unique impacts of each ICO. This empirical

[8] The only exception is ETH, which is typically used as the issuance currency. Hence, treated cyptos excludes ETH.

specification helps rule out many likely sources of estimation bias and confounding effects at the crypto or ICO level, allowing the variations of treated cryptos before and after large ICOs to provide desirable statistics for estimating the impact of ICO-induced congestion.

We observe that treated cryptos exhibit higher *InRanks* and deliver a significantly negative cumulative return of -20.8% in the three weeks following large ICOs. The first effect indicates that large ICOs enhance the capital inelasticity of treated cryptos. The second effect, reflected in returns, validates the asset pricing implications of inelastic crashes. Furthermore, the dynamic treatment effects reveal that *InRank* increases immediately during the ICO week, whereas the significant impact on returns starts one week after the ICO. The time lag between the two dynamic effects is consistent with the notion that heightened inelasticity leads to predictive crashes. In addition, we observe that large ICOs significantly increase the average time between transactions while reducing the number of transactions, confirming that enhanced *InRanks* are associated with more blockchain congestion and reduced trading demand.

An important alternative explanation is that large ICOs may distract investors' attention. As such, inattention, rather than capital inelasticity, could be the main reason for reduced demand and price declines. However, the same DiD test suggests that Google searches increased for treated cryptos during the post-ICO period, making inattention difficult to explain our results. Collectively, our DiD tests support a causal interpretation of the predictive power of capital inelasticity and provide a concrete economic mechanism underlying inelastic crashes.

In addition to inattention, several other economic channels may also be related to observed crash patterns. For instance, Cong, Karolyi, Tang, and Zhao (2023) suggest that the growth rate of addresses with balance and the value effect (proxied by the negative of the past 52-week return) may influence crypto pricing. Moreover, extreme returns naturally indicate high volatility. Although our tests account for idiosyncratic risk and volatilities associated with common factors, volatility timing could still influence portfolio returns over time (Asness, Frazzini, and Pedersen, 2012; Moreira and Muir, 2017). Next, the prospect theory helps reconcile anomalies (Barberis, Mukherjee, and Wang 2016; Barberis, Jin, and Wang 2021), which may also apply to crypto-return dynamics. Lastly, maximum daily returns (Bali, Cakici, and Whitelaw, 2011) may be related to our measures of *MaxRunup* and *MaxDrawdown*, potentially influencing our results.

Despite the importance of these alternative channels, our further analysis suggests that they do not undermine the return predictive power of capital inelasticity. It is also worth noting that the sequence of price changes—whether the *MaxRunup* precedes the *MaxDrawdown* or vice versa—has no impact on our conclusions. In other words, inelastic crashes are equally likely to occur after significant positive or negative price movements. This irrelevance suggests that our results are unlikely to be influenced by recency bias, extrapolation, or persistently biased beliefs about the fundamental values of these assets.

Lastly, we provide a list of additional analyses to provide further economic insights into our main findings. We first ask whether inelastic crashes are confined only to small cryptos. To this end, we show that the pricing power of *InRank* remains highly significant among the top 500 cryptocurrencies, suggesting that congestion-induced inelastic crashes are common across blockchain-based assets regardless of size. Another important question is whether new developments in blockchain could alter our results. Specifically, third-generation blockchain innovations, such as those introduced by EOS, aim to enhance transaction speeds. However, inelastic crashes remain significant for both subsamples before and after the advent of EOS (including EOS), suggesting that the new blockchain technologies do not fully address the issue of capital inelasticity. Moreover, cryptos are often classified as coins or tokens, depending on whether they operate on their own blockchains. Our findings indicate that both categories exhibit inelastic crashes.

Our paper speaks to several strands of the literature. Recent studies examine different pricing aspects of cryptocurrencies to infer the underlying mechanisms and economic implications. For instance, researchers link cryptocurrencies to anomalies (Hubrich, 2017; Rohrbach, Suremann, and Osterrieder, 2019), bubbles and crashes (Corbet, Lucey, and Yarovaya, 2018), factor models (Liu and Tsyvinski 2021; Liu, Tsyvinski and Wu, 2022; Cong, Karolyi, Tang and Zhao, 2023), and market frictions (Makarov and Schoar, 2020; Borri and Shakhnov, 2022).[9] Our analysis of inelastic crashes extends these efforts and differs from known theories on cryptos. For instance, existing studies view crypto crashes as a sunspot, which is extrinsically random, or attribute them to the risk of flawed protocol or attacks (e.g., Garratt and Wallace, 2018; Biais et al., 2023). Investor belief about crypto's future value and adoption (e.g., Benetton and Compiani, 2021; Kogan,

[9] A few recent studies model the exchange rates of cryptocurrencies (Bolt and van Oordt 2020), the influence of cost of production (Hayes 2017), investor attractiveness (Ciaian, Rajcaniova and d'Artis Kancs 2016), as well as market designs related to trading (Katya and Park 2017), transaction fees (Easley, O'Hara, and Basu, 2019), and information disclosure (Cong and He, 2019). Empirical studies also explore the sensitivity of Bitcoin/USD exchange rate to economic fundamentals and technological factors (Li and Wang 2017), the price efficiency of Bitcoin (Urquhart 2016; Ghysels and Nguyen 2019), price manipulation in Bitcoin trading (Griffin and Shams 2020; Gandal, Hamrick, Tyler Moore, and Oberman 2018), as well as the network effect (Gandal and Halaburda 2016; Cong, Li, and Wang 2021) and membership/fee considerations (Sockin and Xiong 2023b).

Makarov, Niessner, and Schoar, 2022) also helps explain returns.

However, random sunspots cannot be the main mechanism of our findings because our inelastic crashes are predictive. In addition, our measure of *InRank* builds on both large price runups and drawdowns, with the sequence of the two price movements playing an insignificant role. As such, expected (negative) values cannot explain its predicting power. Instead, we propose a new mechanism based on slow-moving capital in inelastic markets (among others, Rubinstein and Wolineky, 1985; Duffie, Gârleanu, and Pedersen, 2007; Duffie, 2010; Koijen and Yogo, 2019; Gabaix and Koijen, 2021). Due to limited blockchain capacity, network delay, and settlement waiting time (Sokolov 2021; Hinzen, John, and Saleh 2022; Hautsch, Scheuch, and Voigt 2024), cryptos provide an ideal testing ground to investigate the properties of inelastic capital. We show that an additional assumption of capital inelasticity reducing investor demand suffices to create a new set of asset pricing dynamics, such as inelastic crashes and elastic momentum. We also propose a novel measure to test these predictions.

Our results are also related to the literature on crashes and momentum. Greenwood, Shleifer, and You (2018) and Greenwood et al., (2022) show that industry crashes and financial crises can be predicted using a list of economically motivated yet sophisticated characteristics. Ibragimov, Parlour, and Walden (2024) propose a pricing framework for assets with unobserved, time-varying yields and crash risks for cryptocurrencies. Unlike these approaches, we hypothesize and test the implications of crypto crashes based on inelastic capital. As for momentum, its economic sources are still under debate.[10] Notably, crypto investors adopt momentum-like strategies (Kogan et al., 2024), plausible because of the positive network feedback effects (Cong et al., 2021; Sockin and Xiong 2023a). We show that capital inelasticity might offer a novel and powerful economic foundation for decoding crypto momentum.

The remainder of the paper proceeds as follows. Section II presents our variables and summary statistics. Section III reports the baseline relationship between inelasticity and cryptocurrency crashes. Section IV relates our inelasticity measure to momentum to explore its

---

[10] Barberis et al., (1998), Daniel et al., (1998), Hong and Stein (1999), and Grinblatt and Han (2005) argue that momentum can be generated by behavioral biases. Berk et al., (1999), Johnson (2002), and Sagi and Seasholes (2007), on the other hand, provide rational explanations. Momentum may also be related to distress risk (Garlappi and Yan, 2011; and Agarwal and Taffler, 2008), long-term risk (Zurek, 2008), the cultural difference (Chui et al., 2010) and institutional investors (Vayanos and Woolley, 2013). Stock momentum is known to be contingent on market conditions (Cooper et al., 2004; Stivers and Sun, 2010) and influenced by time-varying attributes such as market betas (Grundy and Martin 2001), market timing (Daniel and Moskowitz, 2016), and factor momentum (Lewellen 2002; Ehsani and Linnainmaa 2022; Arnott et al., 2022).

asset pricing implications. Section V presents the results of a difference-in-difference test to investigate the mechanism based on Ethereum ICOs. Section VI provides additional analysis and robustness checks, and a brief conclusion follows.

II. Data and Main Variables

A. Sample and Data Sources

Trading data are collected from "Coinmarketcap.com." Coinmarketcap.com is one of the most-referenced price-tracking websites for crypto assets. To be listed in Coinmarketcap.com, a cryptocurrency must fulfill specific criteria, including possessing a solid technical foundation, a functional website, a block explorer, and actively being traded on at least one exchange (with material volume) that has maintained a tracked listing status on Coinmarketcap. We download the daily data of close price, trading volume, and market capitalization in USD for each cryptocurrency listed on the website from April 28, 2013 to May 12, 2024. According to Coinmarketcap.com, the price is calculated as a volume-weighted average of the reported market pair prices across various markets. The trading volume represents the aggregate spot trading volume reported by all exchanges. The market capitalization is calculated by multiplying the existing reference price of the cryptocurrency by the current circulating supply.

Our initial dataset consists of 26,127 cryptocurrencies. Since the trading volume data became available in the last week of 2013, we restrict our sample to start from the start of 2014 to May 12, 2024. We require cryptocurrencies to have price, volume, and market capitalization information. For each week t, we further exclude coins with market capitalization at the end of week t-1 less than $1,000,000 following Liu et al., (2022) and coins with a trading volume of less than one dollar during week t-1 to exclude the extremely illiquid coins[11]. We exclude each cryptocurrency's first week of trading return to mitigate any potential issues associated with Initial Coin Offerings (ICOs). Weekly returns are winsorized at 0.1% and 99.9%[12] to address outliers and potential data errors. However, our main results remain similar without winsorizing the returns. We also require that the cryptocurrencies have trading data from the start of week t-12 to the end of week t-1 at each week

[11] We also exclude Innovative-Bioresearch-Classic, the market capitalization of which reached $29,328 trillion, following Cong et al., (2023).

[12] Some cryptocurrencies earned extreme returns, even above 1000 in week t, with more than $1,000,000 market capitalization at the end of week t-1. These outliers could lead to serious estimation errors, empirically. Borri et al., (2022) also use the winsorization method when analyzing returns of NFTs (Non-Fungible Tokens).

t to construct our measures of inelasticity. After applying these filters, our sample consists of 4,284 cryptocurrencies. We also collect Google Search data from Google Trends to proxy investors' attention.

We obtain the on-chain data of cryptocurrencies from Intotheblock.com (comprising 747 cryptocurrencies), following Cong et al., (2023) and Liu and Tsyvinski (2021). From Intotheblock, we gather the Average Time between Transactions, Number of Transactions, Active Addresses, and Total Addresses with Balance from both databases. Upon merging this augmented on-chain data with our existing trading data, the resulting dataset encompasses 581 cryptocurrencies (as summarized in Table 1).

Lyandres et al., (2022) have established a comprehensive and publicly available ICO database covering over 5400 completed ICOs from 11 ICO data sources from 2015 to 2019. We further complement the ICO data from ICOdata[13] and Coinmarketcap since 2020 and calculate the raised amount by converting it to USD. To determine the public blockchain the cryptocurrencies build on, we first check the public chain information in Intotheblock. If Intotheblock does not cover the cryptocurrency, we subsequently check the contract information in Coinmarketcap and Etherscan.io. We also include cryptocurrencies using multiple public chains in our ETH-based sample if they are built on the Ethereum Chain. Finally, our ICO dataset contains 4,715 ICOs built on the Ethereum Chain from Oct 2015 to May 2024.

All the non-return characteristics of cryptocurrencies, including size (logarithmic market capitalization), Ret [a, b] (cumulative returns from the start of week *a* to the end of week *b*), turnover ratio (the average of daily turnover ratio in the past 12 weeks prior to week *t*), lnAmihud (logarithmic average of daily Amihud illiquidity ratio in the past 12 weeks prior to week *t*), IVOL (idiosyncratic volatility in the past 12 weeks prior to week *t*), skewness and kurtosis of returns in the past 12 weeks prior to week *t*, value (the negative of cumulative 52-week returns prior to week *t*), network (the logarithmic growth rate of total addresses with balances at week *t*-1), average time between transactions (past 12-week average), number of transactions (past 12-week average), total addresses with balances (past 12-week average), active addresses (past 12-week average), and Google Search (past 12-week sum) are winsorized at 1st and 99th percentile. The summary statistics

[13] This dataset has been used by Sokolov (2021). This dataset does not include the start date of ICOs. In this sample, we use the exchange rate of the cryptocurrencies or currencies received in ICO at the end date of ICOs to convert the raised amount into US dollars. We manually complement the missing information on the ICO start date in this dataset.

of these variables are shown in Table 1. We replicate the Crypto-three-factor and Crypto-five-factor models following Liu, Tsyvinski, and Wu (2022) and Cong, Karolyi, Tang, and Zhao (2023), respectively, and present the summary statistics in Table A1.

B. Inelasticity Measure

Our Inelasticity measure is constructed as follows. Firstly, we define the *MaxRunup* and *MaxDrawdown* of cryptocurrency returns. At the end of week t-1, we collect the lowest price (P_{min}) and the corresponding trading date ($Date_{min}$) for each cryptocurrency within the past 12-week period. If the price hits the same lowest value multiple times, we confirm the latest date as $Date_{min}$. To calculate the annualized rate of price change (runup), we use the formula $\left(\frac{P_{t-1}}{P_{min}} - 1\right) * \frac{365}{\#Days}$, where P_{t-1} represents the close price at week t-1. The expression $\#Days$ indicates the number of days from $Date_{min}$ to the end of week t-1.

Similarly, we compute the annualized rate of price change for *MaxDrawdown* using the formula $\left(\frac{P_{t-1}}{P_{max}} - 1\right) * \frac{365}{\#Days}$, where P_{t-1} represents the close price at week t-1. Here, the expression $\#Days$ denotes the number of days from $Date_{max}$ to the end of week t-1.

We further get the cryptocurrencies' ranks for the *magnitude* of their *MaxRunup* and *MaxDrawdown*. These ranks are then divided by the total number of cross-sectional observations to standardize the *MaxRunup* and *MaxDrawdown* measurements within the range of [0, 1]. We denote these standardized values as $Rank_{runup}$ and $Rank_{drawdown}$.

The concept of inelasticity implies that cryptocurrency prices are susceptible to both significant runups and drawdowns. In order to capture this behavior, our main proxy for capital inelasticity, *InRank*, is defined as $(Rank_{runup} + Rank_{drawdown})/2$. For easy interpretation, we further normalize *InRank* to have a uniform distribution between 0 (lowest) and 1. To further assess the robustness of our results, we also construct an alternative measure of inelasticity denoted as $Inelasticity_{pro}$, which is the product of $Rank_{runup}$ and $Rank_{drawdown}$. We utilize these two Inelasticity measures' uniformly standardized cross-sectional ranks in our empirical tests.

C. Summary Statistics

Table 1 tabulates the summary statistics. Panel A shows that the number of coins in our dataset has increased significantly, from 62 in 2014 to 2,324 in 2021, and then decreased to 1,798 in 2014. We observe a substantial growth in the number of coins, market capitalization, and trading volume during two distinct periods: from 2016 to 2017 and from 2020 to 2021. At the end of our sample period, market capitalization's mean (median) value rises to 1454.54 (21.72) million dollars.

Panel B reports the distribution of the main characteristics of cryptocurrencies in our sample, including returns, logarithm of market capitalization (Size), logarithm of Amihud illiquidity ratio (lnAmihud), Turnover, idiosyncratic volatility (IVOL), non-annually *MaxRunnup* and *MaxDrawdown*, the negative of past 52-week cumulative returns (Value), the log difference of total address with balance (BA growth). The average weekly return of a typical cryptocurrency in our sample period is approximately 1%, with a standard deviation of 0.27. The 75th percentile of *MaxRunnup* and the 25th percentile of *MaxDrawdown* were 0.32 and -0.90, respectively. The high standard deviation and substantial extreme values suggest that cryptocurrencies are subject to large price movements, highlighting the importance of bubbles and crashes in the crypto market. Our online appendix (Table A1) provides additional summary statistics for crypto factors and network characteristics.

III. Capital Inelasticity and Crashes

In this section, we examine the relationship between capital inelasticity and crashes. We offer two diagnostic tests to validate the economic interpretation of our inelasticity measure, followed by a formal investigation of inelastic crashes.

A. Inelasticity and Blockchain Network Characteristics

We first utilize the subsample of cryptos with blockchain information to conduct the following diagnostic test in panel specifications:

$$\begin{aligned} InRank_{i,q} = a + \beta_1 \times Time_{i,q} + \beta_2 \times \#Transaction_{i,q} + \gamma \times Time_{i,q} \times \#Transaction_{i,q} \\ + C \times M_{i,q} + v_i + u_q + \varepsilon_{i,q}, \end{aligned} \quad (1)$$

where $InRank_{i,q}$ refers to the capital inelasticity of cryptocurrency i in a non-overlapping quarter q (i.e., a 12-week, $Time_{i,q}$ refers to the average time between transactions, $\#Transaction_{i,q}$ is the number of transactions, and the vector $M_{i,q}$ consists of variables to control for the capacity of the blockchain, including the number of active addresses (*#ActAdr*) and the number of addresses with balance (*#BA*). All network variables are measured as the logarithm of the average values over the past quarter (i.e., 12 weeks). We also use a non-overlapping sample to deal with the potential residual autocorrelation. We further control for the coin- and time-fixed effects or, alternatively, a more restrictive blockchain × time fixed effects.

We focus on two parameters from the regression, β_1 and γ. Specifically, β_1 is of particular interest because a longer *Time* reduces the speed at which capital can participate in trades, thereby enhancing network delay and settlement waiting time (Hinzen, John, and Saleh 2022; Hautsch, Scheuch, and Voigt 2024). In this context, *Time* serves as a direct proxy for blockchain-based, slower-moving capital. Consequently, the coefficient β_1 indicates the extent to which our measure ($InRank_{i,q}$) captures capital inelasticity. Note that the sign of β_2 is less clear *ex ante*. An increase in realized transactions could suggest improved liquidity conditions ($\beta_2 < 0$) if these trades originate from enhanced participation by liquidity providers, or from disagreements among a broader scope of investors (e.g., Hellwig, 1980; Kim and Verrecchia, 1994). However, trading volume may also be stimulated by informed investors (Grossman and Stiglitz, 1980; Kyle, 1985). Since the trading activities of these investors demand liquidity, they could exacerbate blockchain congestion when the capital of liquidity providers only partially participates in the market ($\beta_2 > 0$).

Despite the ambiguity of β_2, we expect γ to be positive if our measure ($InRank_{i,q}$) properly describes capital inelasticity. This is because, during periods of congestion (i.e., conditioning on a high value of *Time*), increased trading demand is likely to further worsen network and settlement delays as more capital competes for limited blockchain resources. This effect arises regardless of the type of demand and aligns with the theoretical prediction that constraints on transaction rates, combined with increased transaction demand, will lead to larger price responses on the blockchain (Hinzen, John, and Saleh, 2022). Within our framework, this dynamic can generate more substantial price jump-reversal patterns as captured by $InRank_{i,q}$.

The results are tabulated in Table 2. We find that both β_1 and γ are significantly positive. Hence, our measure ($InRank_{i,q}$) is positively associated with both blockchain processing time and its interaction with the number of transactions. These contemporaneous relationships remain significant even after controlling for other important blockchain properties, such as active addresses and addresses with balance (Cong et al., 2023; Irresberger et al., 2021), and under highly restrictive fixed effects in column (4). These findings suggest that our measure generally reflects the blockchain trading frictions that slow down the speed of capital. Interestingly, we observe that β_2 is also significantly positive, indicating that increased trading activity on the blockchain generally amplifies capital inelasticity rather than enhancing liquidity provision.

B. Diagnostic Analysis on MaxRunnup and MaxDrawdown

Our second diagnostic analysis aims to investigate how *MaxRunup* and Max*Drawdown*, the two components of *InRank*, are associated with crypto crashes. To achieve this goal, we independently sort cryptocurrencies into three bins (30%-40%-30%) at the start of each holding week based on their *MaxRunnup* and *MaxDrawndown* values, measured during the prior 12-week (quarterly) ranking period. These portfolios are held for one week and rebalanced weekly. We then report value-weighted returns for cryptocurrencies within these double-sorted portfolios, along with their adjusted performance based on one-factor, three-factor (Liu, Tsyvinski, and Wu, 2022), and five-factor models (Cong, Karolyi, Tang, and Zhao, 2023). The summary statistics for the sorting variables are provided in our Online Appendix (Table A2).

The results are tabulated in Table 3. Specifically, Panel A details the performance of each double-sorted portfolio. Panel B further reports the differences between these portfolios with respect to the mid/mid portfolio. We first observe that high *MaxRunup* ranks do not lead to high returns. This observation is surprising based on the prevalence of crypto momentum: i.e., *MaxRunup* implies a high ranking period return, which should deliver a high holding period return according to momentum. Instead, within portfolios with the highest *MaxDrawndown* values, the portfolio with the highest *MaxRunup* values appears to have a lower return or risk-adjusted performance than the portfolio with the lowest *MaxRunup* values.

Indeed, the portfolio with the highest *MaxRunup* and highest *MaxDrawndown* (i.e., the top/top portfolio) delivers the lowest performance among all portfolios. Not only does the portfolio deliver negative performance, it also significantly underperforms the mid/mid group by a spread of -2.6% in excess returns, or -2.3% and -2.1% adjusted returns by the three-factor five-factor models. Our online appendix (Table A3) shows that similar underperformance is observed even when we hold the double-sorted portfolios for longer holding periods, such as 4 weeks or 8 weeks.

Easy to see, cryptos in the top/top portfolio have the highest *InRank* values among all assets. Since *MaxRunnup* and *MaxDrawndown* cannot occur simultaneously on the same date, what these cryptos experience during the ranking period is the sequential occurrence of large price movements with opposite signs, characterizing a jump-reversal pattern. Therefore, our second diagnostic analysis suggests that *InRank* values from the ranking period can serve as a predictive indicator for crashes during the holding period.

C. The Return Predictive Power of InRank

Thus far, our diagnostic tests suggest that *InRank* aligns closely with indicators of inelastic capital and that its two components can jointly predict crashes. These observations suggest that *InRank* provides a reasonable metric for testing the asset pricing implications of inelastic capital.

We now more formally investigate the return predictive power of inelastic capital. To this end, we provide both portfolio analyses and multivariate regressions. In portfolio analysis, we sort cryptocurrencies into quintile portfolios based on their quarterly ranking-period *InRank* values, and we rebalance these portfolios weekly. We also construct a value-weighted Elastic-minus-Inelastic (EMI) portfolio that longs the cryptocurrencies in the elastic (bottom inelastic) quintile and shorts the most inelastic quintile. We then report value-weighted returns for cryptocurrencies within these portfolios, along with their adjusted performance based on one-factor, three-factor, and five-factor models.

We tabulate the characteristics of these sorted portfolios in Table 4, Panel A for performance and Panel B for other properties, including Size, illiquidity (Amihud), Turnover, Ivol, Skewness, and Kurtosis. From Panel A, we observe that high capital inelasticity is in general associated with lower returns. Moreover, the EMI portfolio can generate a significant weekly return of 2.5%, which remains as high as 2.6% and 2.4% when adjusted by the three and five-factor models. This spread quantifies the return impact associated with capital (in)elasticity. The last two columns of Panel A extend the EMI holding period to 4 and 8 weeks. We observe that the economic magnitude and statistical significance of the EMI spread remain highly robust.

Panel B reports that EMI is positively associated with size and negatively associated with illiquidity, Turnover, Ivol, Skewness, and Kurtosis. The significance of these characteristics suggests that a more thorough analysis of EMI returns should control for their impact. As a result, we next use multivariate analysis to assess the return predictability of capital inelasticity.

More specifically, we estimate the following weekly Fama-MacBeth regressions:

$$Ret_{i,t} = \alpha_t + \beta \quad \times InRank_{i,t-1} + \gamma \times X_{i,t-1} + \varepsilon_{i,t}, \tag{2}$$

where $Ret_{i,t}$ refers to the return of the crypto i in week t, $InRank_{i,t-1}$ is capital inelasticity estimated in the quarterly ranking period prior to week t, and the vector $X_{i,t-1}$ stacks a list of control variables, including two-week momentum (Ret [-2, -1]), Size, lnAmihud, Turnover, cumulative returns from t-12 to t-3 (Ret [-12, -3]), IVOL, Skewness, and Kurtosis.

The results are presented in Table 5. The first three columns report the return predictive power of $InRank_{i,t-1}$, while columns (4) through (6) replace $InRank_{i,t-1}$ with a dummy variable indicating cryptos with the most severe (i.e., top 20%) capital inelasticity in the cross section prior to week t. We observe that both *InRank* and *Inelasticity Dummy* predict significantly negative future returns. To illustrate the economic magnitude of this effect, consider column (3), where the regression coefficient for *InRank* is -0.055. Given the standard deviation of *InRank* is 0.2887, a one-standard-deviation increase *InRank* is associated with -1.59% weekly returns ($= -0.055 \times 0.2887$). Moreover, columns (4) through (6) suggest that 20% of most inelastic cryptocurrencies are associated with more negative out-of-sample weekly returns, ranging between -1.2% and -2.5%. These estimates are substantial and align well with the outcomes of our portfolio analysis.

The predicting power is not absorbed by known cryptocurrency factors, such as market, size, and momentum, or investor's preference over idiosyncratic volatility and lottery payoffs. Our results are also robust when controlling for the traditional liquidity measures, such as the Amihud illiquidity ratio and turnover ratio, suggesting that our proxy for inelasticity capital adds new information above these illiquidity measures. Collectively, both portfolio and regression analyses support the notion that capital inelasticity predicts crashes.

Instead of using negative returns as a proxy for crashes, we can also directly link dummy indicators of crashes to capital inelasticity based on the following panel specification:

$$D_{i,t+h-1}(Crash) = \alpha_0 + \beta_1 \times InRank_{i,t-1} + c \times X_{i,t-1} + \varepsilon_{i,t+h-1}, \tag{3}$$

where $D_{i,t+h-1}(Crash)$ is a dummy variable indicating the occurrence of a crash (i.e., the occurrence of a large bottom-quintile price drawdown) for cryptocurrency i from week *t* to week $t + h - 1$ (*h* = 1, 4, and 8). Other variables are similar to the return analysis.

Table 6 reports the results for two versions of the above equation, an OLS panel regression in

Panel A and a panel logistic regression in Panel B. In the linear model (Panel A), the standard errors are calculated using Driscoll and Kraay (1998) methodology with lags of (2, 6, 12) for h=1,4,8, and the p-values are adjusted following Kiefer and Vogelsang (2005), as applied by Greenwood et al., (2022). For the panel logistic regression in Panel B, standard errors are clustered at the cryptocurrency level.

Across both panels, capital inelasticity is positively associated with the out-of-sample crash dummy. For example, column (2) of panel A reports that the top 20% of most inelastic cryptocurrencies are associated with an 8.7% higher likelihood of crash. In column (2) of Panel B, these cryptocurrencies are associated with 8.02% higher probability of a crash.[14] These findings consistently demonstrate that capital inelasticity is a significant predictor of crash risk.

We perform several robustness checks on the above result (tabulated in our online appendix). In Table A4, we use alternative specifications, such as controlling for time-fixed effects, controlling for the large drawdowns and large runups, and using net crashes (the crypto experiences a crash but not a bubble) as the dependent variable. In Table A5, we use a non-overlapping sub-sample to deal with the potential residual autocorrelation not fully captured by Driscoll and Kraay's (1998) adjustment. Our findings remain robust across these settings, indicating that unobservable common shocks, conventional reversals or momentum effects, or residual autocorrelation are unlikely the main driving forces for our main observations.

IV. Asset Pricing Implications on Momentum

Perhaps the most interesting asset pricing implication of capital inelasticity is momentum. In this section, we first show that the effect of crypto momentum depends on capital elasticity. Next, we construct an *ElasticWinner-Minus-InelasticLoser* (EWIL) strategy, which can outperform momentum and generate positive returns up to 52 weeks of the holding period. We also compare the crash risks of momentum and EWIL to understand the economic interpretation of the latter.

A. Momentum and Inelasticity in Double-sorted Portfolio

[14] The average of semi-elasticity is defined as $E[e_{i,t}] = E\left[\frac{\partial ln\Pr[y_{i,t} = 1|x_{i,t}, \alpha_i]}{\partial x_{i,t}}\right]$. Therefore, the results indicates that the top 20% of most inelastic cryptocurrencies are associated with a 40.1% increase in the conditional probability of a crash, $ln\Pr[y_{i,t} = 1|x_{i,t}, \alpha_i]$. Since the unconditional probability of a crash is 20%, the absolute magnitude is 8.02%, which is close to 8.7% in the linear model.

Vast studies show that crypto momentum can generate significant excess returns and help explain the cross-section of expected returns (Liu and Tsyvinski, 2021; Liu, Tsyvinski, and Wu, 2022; Cong, Karolyi, Tang, and Zhao, 2023). Liu, Tsyvinski, and Wu (2022) further show that the momentum strategy is markedly stronger among the large and well-known coins, followed by a reversal, consistent with the attention-based overreaction-induced momentum effect.

Our new intuition is that capital inelasticity and its associated inelastic crashes may directly affect momentum. Especially, capital inelasticity may invalidate momentum on the winner side: if the high returns of some past winners originate from inelastic capital—i.e., inelastic winners, the heightened risk of subsequent inelastic crashes could offset the continuation of positive returns. Conversely, inelastic crashes and momentum may join forces to produce more enduring negative returns. These considerations suggest that momentum may perform well among elastic cryptos (i.e., *elastic momentum*) but not necessarily in inelastic ones. Indeed, if the impact of inelastic crashes on momentum winners exceeds that on losers, momentum returns may diminish among inelastic cryptos.

To investigate the momentum impact of inelasticity, we double-short cryptocurrencies into three groups (using 30%-40%-30% splits) based on their past two-week returns and *InRank* estimated during the quarterly ranking period prior to the holding week. These portfolios are held for one week and rebalanced weekly. Again, we report value-weighted returns for cryptocurrencies within these double-sorted portfolios and their adjusted performance based on one-factor, three-factor, and five-factor models. We further construct value-weighted winner-minus-loser portfolios (WML) across *InRank* groups and value-weighted elastic-minus-inelastic portfolios (EMI) across momentum groups.

Table 7 presents the double-sorting results. Consistent with the literature, we observe significant momentum returns. Specifically, the WML strategy can generate a significant weekly return of 1.3% among all cryptos and 2.1% among the most elastic ones. Adjusting for factor models slightly reduces the economic magnitudes. Nonetheless, momentum returns remain highly robust in our sample period.

Our new observation is that WML fails to deliver positive returns among the most inelastic cryptos. This insignificance arises from two EMI effects. First, EMI can generate a significantly positive weekly return of 2.7% among past winners. Put differently, inelastic winners underperform elastic winners, with an economic magnitude comparable to elastic momentum and even larger than general momentum. Second, EMI results in insignificant returns among past losers. While inelastic losers also tend to underperform elastic losers, the return difference is modest at only 0.8%. As a result, inelastic winners fail to outperform inelastic losers. Collectively, the return impact of inelastic crashes on winners is substantially larger than the impact on losers, leading to the diminishment of inelastic momentum returns.

The above patterns suggest that the *ElasticWinner-minus-InelasticLoser* (EWIL) strategy could help deliver higher returns than traditional momentum. We next conduct a portfolio analysis to test this prediction. To prioritize the importance of capital inelasticity, we first sort cryptos into three groups (30%-40%-30%) according to their *InRanks*. Within each group, we further divide assets into three groups (30%-40%-30%) according to their past two-week returns. The *EWIL* portfolio is then created by taking long positions in Elastic-Winners and short positions in Inelastic-Losers.

We observe that the EWIL strategy generates a weekly return of 3.4%. The three-factor and five-factor model-adjusted alphas are also sizable, 3.3% and 3.2%, respectively. Table A6 confirms that the results remain robust for independent sorted EWIL, though the economic magnitude is slightly smaller. It is worth noting that the magnitude of EWIL returns almost triples that of general momentum. Even when compared to the higher return of elastic momentum, EWIL outperforms by approximately 62%.

B. Bear Market Betas of EWIL

Momentum strategies in the stock market are subject to crash risks (Daniel and Moskowitz, 2016). Momentum crashes occur during bear markets because momentum behaves like written call options on the market, resulting in significant losses when the market rebounds (Daniel and Moskowitz, 2016). This phenomenon is analogous to negative market timing. Considering the high returns generated by EWIL, a natural question arises: is this performance compensation for heightened crash risk?

To address this question, we investigate the crash risks in the following regression following Daniel and Moskowitz (2016):

$$\tilde{R}_t = (\alpha_0 + \alpha_B \times I_{B,t-1}) + (\beta_0 + I_{B,t-1}(\beta_B + \tilde{I}_{U,t}\beta_{B,U})) \times \tilde{R}_{Mkt,t} + \tilde{\epsilon}_t, \quad (4)$$

where the key dependent variable $\tilde{R}_t$ is the return of a particular portfolio (e.g., momentum or EWIL) in week t, $\tilde{R}_{Mkt,t}$ represents the market-capitalization-weighted (VW) index of all the cryptocurrencies in week t, $I_{B,t-1}$ denotes an ex-ante bear market indicator that equals one if the cumulative VW index return in the past 4 weeks is negative and is zero otherwise, $I_{U,t}$ is a contemporaneous, i.e., not ex-ante, up-market indicator variable that is one if the excess VW index return is greater than the risk-free rate in week *t*, and is zero otherwise. Given that the duration of crashes in the cryptocurrency market is not as long as the equity market, the down-market is estimated as a negative market return in the 4 weeks prior to the holding period.

In this specification, α_0 and α_B denote the abnormal return of the portfolio in general and during the downside market in particular. In line with the two performance measures, the parameters β_0 and β_B capture the portfolio's exposure to the market in general and during the bear market in particular. The parameter $\beta_{B,U}$ measures whether the portfolio has a positive market timing ability during the downside of the market. A negative $\beta_{B,U}$ indicates negative market timing, while a positive β_B reflects enhanced market exposure during the bear market. Both scenarios suggest heightened downside risk for the underlying trading strategy.

We apply the above test to the three strategies of momentum, EMI, and EWIL. The results are reported in Table 8. Columns (1) to (3) reports α_0, alphas adjusted only by the market. We observe that all these three strategies deliver significant market-adjusted returns. Columns (4) to (6) present the estimates of the specification in Equation (4). For crypto momentum, $\beta_{B,U}$ is negative yet insignificant, suggesting that the crypto moment has negative yet marginal optionality. However, β_B is highly significant, indicating that its market exposure increases significantly during the bear market. Taken together, crypto momentum has significant exposure to crash risk through its enhanced market exposure during the bear market.

EMI and EWIL behave very differently. EMI has insignificant $\beta_{B,U}$ or β_B, suggesting that this strategy is not exposed to the downside risk that momentum typically exhibits. More interestingly, EWIL exhibits positive $\beta_{B,U}$, or positive market timing during bear markets. This suggests that EWIL benefits from the risk of market crashes by shorting inelastic losers. As a result, EWIL return is not a compensation for crash risk commonly observed in equity and currency momentum

(Daniel and Moskowitz 2016).

C. The Dissipation of Inelasticity (EWIL)

Finally, we investigate the effective duration of EWIL. Since markets with inelastic capital require more time to reach equilibrium, we hypothesize that EWIL will deliver higher returns over more extended holding periods than traditional momentum. To evaluate this hypothesis, we compute the cumulative returns for both EWIL and WML across holding periods of up to 52 weeks.

Figure 2 illustrates the returns achieved across varying holding period lengths. We observe that momentum returns peak at a holding period of 9 weeks and then decline as the holding period extends further. Eventually, its returns turn negative when the holding period exceeds 20 weeks. In contrast, EWIL returns continue to increase over extended holding periods and show no signs of dissipation, even with a holding period of up to 52 weeks. This slow dissipation indicates that the impact of inelastic capital is highly persistent within the market.

As EWIL is unexplained by common crypto factors and uncorrelated with crash risk, both the magnitude and extended duration of EWIL returns may seem surprising. These characteristics suggest prolonged periods of price inefficiency and arbitrage opportunities, far exceeding the duration of well-documented anomalies like momentum. However, such properties align with theories of slow-moving capital and unveil new insights into the crypto market. Dow, Han, and Sangiorgi (2021) show that, in a market with slow-moving capital, shocks in price inefficiency can deplete arbitrage capital, leading to hysteresis inefficiency. Our results align with this theoretical framework. Specifically, when blockchain congestion leads to price inefficiency due to capital inelasticity (i.e., high *InRank*), investors reduce their demand and capital even further, exacerbating price inefficiency through inelastic crashes and resulting in extensive EWIL returns.

Capital inelasticity also introduces a novel source of risk for (buy-side) momentum. As discussed by Cong, Li, and Wang (2021), network adoption fueled by price increases can generate additional network externalities, leading to feedback effects and price momentum. Kogan et al., (2024) observe that retail investors appear to adopt this framework in their crypto trading, which differs significantly from their behavior in stock trading. Our findings offer new insights into the origins of crypto momentum. In our framework, inelastic crashes contradict buy-side momentum while amplifying sell-side momentum. From a network feedback perspective, elastic capital fosters positive network feedback effects. In contrast, inelastic capital amplifies momentum's negative impact on prices and price efficiency. Overall, our findings indicate that blockchain-induced capital inelasticity can play a critical role in shaping asset prices and momentum-related anomalies.

V. Mechanism Analysis based on Ethereum ICOs

Thus far, our empirical findings support the concept of inelastic crashes and their impact on momentum. In this section, we conduct an identification test to examine the blockchain-based mechanism of capital inelasticity, using data from the 50 largest Initial Coin Offerings (ICOs) conducted on the Ethereum blockchain.

A. Ethereum ICOs and Diff-in-Diff Tests

Our ICO dataset contains 4,715 ICOs built on the Ethereum Chain[15] from Oct 2015 to May 2024. According to our ICO dataset, Ethereum witnessed a surge of ICO activity from September 2017 to June 2018, which then declined significantly. However, the amount of funds raised by ICOs remained high after the drop in ICO numbers, except for a slump in 2020. The fundraising amount reached its peak in 2021. ICO can induce congestion on blockchain. For example, on November 28, 2017, Ethereum was stuck by the ICO of CryptoKitties. The rapid spike in popularity caused Ethereum to become congested and induced extremely high fees. Large ICOs built on Ethereum likely occupy a significant fraction of the trading capacity of the Ethereum blockchain, which introduces plausibly exogenous shocks to crowd out the transaction capacity for other existing cryptos based on Ethereum, except ETH itself, because ETH usually serves as the issuance currency. This mechanism provides a natural treatment group, namely, the other existing cryptos built on Ethereum. The control group consists of cryptocurrencies from non-Ethereum blockchains. Therefore, we can employ a DiD method to examine how ICO-induced blockchain congestion affects crypto inelasticity and future returns.

We employ the top 50 ICOs according to the amount raised in dollars in unit time, i.e., we normalize the amount raised by (ICO amount in dollars/time in days). Our sample, which comprises transaction data, primarily encompasses cryptocurrencies based on Ethereum. The remaining non-Ethereum-based cryptocurrencies are predominantly cryptos with the largest market capitalization, such as Bitcoin, Dash, and EOS. We use the Mahalanobis-Distance-

[15] According to the statistics from ICO Bench, more than 70% of ICO projects are based on Ethereum. See https://icobench.com/stats/ico-statistics/.

Matching (MDM) method to match the Ethereum-based and non-Ethereum-based cryptocurrencies according to the characteristics at the end of week τ-1 (one week before the ICO start week τ), such as Size, Ret [-2, -1], Ret [-12, -3], lnAmihud, Turnover, IVOL, Skewness, Kurtosis, BA growth, and Value. We employ one-to-one nearest-neighbor matching. After matching, we conduct DiD regressions with a window of [-3, +4]:

$$InRank_{i,t} \text{ or } CAR_{i,t} = a + \beta \times Treat_{i,t} + \gamma \times X_{i,t} + u_{i\times Event} + v_{t\times Event} + \varepsilon_{i,t}, \quad (5)$$

where $InRank_{i,t}$ refers to our proxy for capital inelasticity for cryptocurrency *i* in week *t*, $CAR_{i,t}$ is the cumulative returns achieved in [-3, *t*], and $Treat_{i,t} = ETH_i \times After_{i,t}$ is the indicator for the treatment effect, which equals one if the cryptocurrency *i* is based on Ethereum post the start date of ICO events. We control for the characteristics combined with crypto-event fixed effects and week-event fixed effects. The standard errors are double-clustered at the blockchain-event and week levels to account for time-series correlation and cross-sectional correlation.

Table 9 reports the results of the DiD regressions. The first two columns focus on $InRank_{i,t}$, while the next two columns on $CAR_{i,t}$. Columns (1) and (3) report that the inelasticity of treated cryptos increases by 7.6% after large ICOs, associated with a 20.8% decline in cumulative returns. These findings confirm that ICO-induced congestion generates sizable inelasticity and price decline.

Columns (2) and (4) report the dynamic treatment effects, which we estimate from the following specification:

$$InRank_{i,t} \text{ or } CAR_{i,t} = a + \sum_{j=-3, j\neq -1}^{4} \beta_j \times ETH_i \times I\{t = \tau + j\} + \gamma \times X_{i,t} + u_{i\times Event} + v_{t\times Event} + \varepsilon_{i,t}, \quad (6)$$

where $I\{t = \tau + j\}$ are indicators that equal one if the week is *j* week after the ICO events. Figure 3 also plots the dynamic treatment effects. We observe that *InRank* increases immediately during and after the ICO week, while the cumulative returns become significantly negative starting from the week after ICOs. Importantly, we do not observe any significant pre-ICO differences between the treated and control groups, suggesting that the parallel assumption is satisfied.

B. Frictions and Attention

We further employ the DiD approach to examine blockchain-based slow-moving capital, realized demand, and investor attention. During each week of the DiD testing period, we use the average time between transactions (*Time*) to proxy for blockchain-based slow-moving capital. Recognizing that ICO events can cause highly variable trading volume patterns across different cryptocurrencies, we adjust for these effects by subtracting the weekly average number of transactions during the 12 weeks preceding the testing period from the number of transactions observed each week. This adjusted measure is referred to as *AbVolume*. Additionally, we use Google Search around ICO events as a proxy for investor attention. Following the methodology of Cohn et al., (2022), we perform Fixed-effects Poisson regressions on Time and Google Search.[16]

The results are tabulated in Panel B. Consistent with the notion of ICO-induced congestion, large ICOs cause the Ethereum-based cryptocurrencies to wait more time to be recorded into the public blockchain and are transacted less after the ICO events. Meanwhile, the transactions have dropped significantly before the start date of ICOs. These findings imply that ICOs slow down the speed of capital of treated cryptos.

The results, summarized in Panel B, support the notion of ICO-induced congestion. Specifically, large ICOs lead Ethereum-based cryptocurrencies to experience longer waiting times before being recorded on the public blockchain. Additionally, there is a significant decline in transactions for treated cryptos in the post-ICO period. Analysis of dynamic treatment effects further confirms the satisfaction of the parallel trend assumption. In the interest of space, we plot the dynamic treatment effect in Figure IN2 of our Online Appendix. These findings suggest that ICOs slow down the capital movement of the affected cryptocurrencies.

A potential concern is that large ICOs may capture investors' attention, thereby reducing demand and causing negative returns for the treated cryptocurrencies. However, our analysis of Google Search data indicates large ICOs prompt investors to search more actively for existing cryptocurrencies on the Ethereum blockchain. As a result, investor inattention is unlikely the economic ground behind extended execution time and reduced volume.

---

[16] Cohn et al., (2022) suggest that Poisson regression produces valid estimates when the outcome variable is continuous. Besides, the advantages of Poisson regression include (i) valid semi-elasticity interpretations and no assumptions about the relationship between higher-order model error moments and covariates for consistent estimation and (ii) separable and multiplicative group fixed effects.

Collectively, our DiD tests suggest that large ICOs trigger "shocks" of blockchain congestion. This disruption leads the affected cryptocurrencies to exhibit greater capital inelasticity (i.e., higher *InRank*) and lower returns, lending support to the role of blockchain congestion as the underlying economic mechanism driving capital inelasticity and its associated asset pricing implications.

VI. Additional Analysis and Robustness Checks

We lastly conduct a list of additional tests on alternative channels to shed more light on the economics of crypto inelasticity.

A. Alternative Explanations Related to Investor Biases

One potential driver of price inefficiency is behavioral biases. Specifically, biases such as recency bias, extrapolation, and beliefs about crypto fundamentals can serve as alternative explanations for our findings.

To see if these behavioral biases drive our results, we examine whether the sequence of price changes behind *InRank*—i.e., whether the *MaxRunup* precedes the *MaxDrawdown* or vice versa—affects the return predicting power of capital inelasticity. To this end, we link returns to *InRank* and its interaction with a dummy variable indicating that *MaxRunup* proceeds *MaxDrawdown*, labeled *RunupFirst*. The results are tabulated in column (1) of Table 10.

We observe that the interaction term has insignificant predictive power on returns. In other words, inelastic crashes are equally likely to occur after significant positive or negative price movements. On the other hand, recency bias, extrapolation, or persistently biased beliefs about the fundamental values of these assets will likely predict crashes following negative price movement. As a result, these behavioral biases are unlikely to be the main driving force for the return predictive power of capital inelasticity.

B. Alternative Channels Related to Crypto Characteristics

The second broad class of alternative explanations concerns crypto characteristics. For instance, small cryptos may drive price inefficiency and, hence, the return predictive power of capital inelasticity. To address this concern, we hence conduct the Fama-MacBeth regressions using the subsample of the top 500 cryptocurrencies in market capitalization. Column (2) in Table 10 confirms that the predictability remains highly significant within large cryptocurrencies. Table A7 also presents the double-sorted portfolio performance by inelasticity and size or illiquidity. These results indicate that our findings are not driven by the small or illiquid cryptos.

In addition, Cong, Karolyi, Tang, and Zhao (2023) suggest that blockchain characteristics, such as the growth rate of addresses with balance and the value effect (proxied by the negative of the past 52-week return), may be essential for crypto prices. Second, extreme returns necessarily imply high volatility. Although our tests control for idiosyncratic risk- and common factor-associated volatilities, volatility timing may affect portfolio returns in time series (e.g., Asness, Frazzini, and Pedersen 2012; Moreira and Muir, 2017). Thirdly, extreme returns may affect investors' probability weighting, which, together with loss aversion and skewness of asset returns, allows the prospect theory to potentially explain our results (e.g., Barberis, Mukherjee, and Wang 2016; Barberis, Jin, and Wang 2021). Lastly, the joint occurrence of positive and negative extreme returns may be spuriously correlated with the maximum daily return (e.g., Bali, Cakici, and Whitelaw, 2011), which reflects lottery preferences uncaptured by skewness.

If these alternative channels are the main driving force for crypto pricing, the statistical and economic significance of the coefficients on inelasticity will significantly weaken when we include these channels in our analysis. However, our main results remain highly robust when we explicitly control for the growth and value effects of blockchains (Cong, Karolyi, Tang, and Zhao 2023), the prospect theory value (Barberis, Mukherjee, and Wang 2016), the maximum daily return (Bali, Cakici, and Whitelaw, 2011), and an indicator for POW consensus. In the interest of space, we tabulate the detailed results in our Online Appendix (Table A8). Likewise, when we construct volatility-managed portfolios following Moreira and Muir (2017), we find that volatility timing adds little information to our Inelasticity-related strategies. These results are also presented in our Online Appendix (Table A9).

C. Developments in Blockchain Technology

A third category of alternative channels concerns blockchain technology. New developments in blockchain may challenge our findings on capital inelasticity. If so, our analysis may only apply to older but not newer generations of blockchain technology. Specifically, the third-generation blockchain technology initiated by EOS may significantly enhance its scalability.

To address this concern, we split our sample into two subsamples: those issued earlier than EOS and those after EOS (including EOS). Columns (3) and (4) report the return predictive test based on the two subsamples, respectively. We observe that the return predictive power of capital inelasticity remains robust in both subsamples with similar economic magnitude, suggesting that the new blockchain technologies do not fully address the issue of capital inelasticity. Indeed, given the "blockchain trilemma" where consensus mechanisms cannot simultaneously achieve fault tolerance, resource efficiency, and full transferability (Abadi and Brunnermeier 2022), capital inelasticity could remain an issue for blockchain for a long period of time.

From the perspective of blockchain usage, cryptos are also often classified as coins or tokens, depending on whether they operate on their own blockchains. Columns (5) and (6) apply the return predictive test to the two types of cryptocurrencies. We observe that *InRank* can predict negative returns equally well within these two subgroups, suggesting that capital inelasticity is a common property of all blockchain-based assets.

D. Robustness Checks

Lastly, we assess whether our results are also robust using alternative measures of capital inelasticity and alternative empirical specifications.

Our main proxy of capital inelasticity (*InRank*) is calculated as the average ranks of *MaxRunup* and *MaxDrawdown*. An alternative way of constructing this proxy is to use the product of the two ranks. Column (7) reports that the return predictive power of capital inelasticity remains highly robust when we replace *InRank* with this alternative measure.

Another concern is that, since stablecoins often provide an anchoring point for other crypto assets, the impact of capital inelasticity may concentrate on these coins. However, Column (8) shows that our results are robust when including or excluding stablecoins.

Our Online Appendix provides additional analysis. In our main analysis, we employ a quarterly ranking period and a one-week holding period for the EMI strategy to illustrate the return implications of capital inelasticity. Given the importance of this result, Table A10 presents EMI returns under variations in the ranking period (8, 10, 12, 14, and 16 weeks) and the holding period (2, 4, 6, 8, and 10 weeks). We observe that EMI consistently delivers significant returns across these combinations, confirming that the return implications of capital inelasticity are highly robust in the crypto market.

Likewise, our main analysis uses *InRank* to predict one-week ahead returns. Since it takes time for capital inelasticity to achieve equilibrium, we might expect *InRank* to predict out-of-sample returns with longer periods. Table A11 confirms this conjecture. It shows that *InRank* can predict significantly negative four-week or eight-week returns.

VII. Conclusion

Limited transaction processing capacity poses a fundamental technical challenge to blockchain-based financial applications (e.g., Bitcoin) and may significantly impact asset prices by restricting the speed and scale of capital flows. In this paper, we propose that blockchain-induced capital inelasticity can help explain a key phenomenon in the crypto market: frequent and large-scale crashes.

Empirically, using a revealed preference approach, we construct proxies for capital inelasticity and find that inelastic cryptocurrencies underperform elastic ones, reflecting crash risk linked to inelasticity. Notably, the risk of inelastic crashes overrides the momentum effect among inelastic cryptocurrencies. This leads to the phenomenon of elastic momentum, where significant momentum-driven returns occur among elastic cryptocurrencies. In contrast, momentum fails to deliver significant returns among inelastic cryptocurrencies.

Furthermore, we show that the Elastic Winner-minus-Inelastic Loser (EWIL) strategy, which combines inelastic crash risk and elastic momentum, yields higher and longer-lasting returns than traditional momentum. Additional analysis on momentum crashes suggests that capital inelasticity may provide a new source of risk for buy-side momentum. We also analyze ICO-induced Ethereum blockchain congestion to provide causal evidence for our proposed mechanism.

Overall, our findings hold important normative implications, suggesting that constrained transaction capacity and slow-moving capital may impose fundamental limits on price efficiency in cryptocurrency and blockchain-based markets.

References

Abadi, J., & Brunnermeier, M. (2022). Blockchain economics. *NBER Working Paper Series*.

Agarwal, V., & Taffler, R. (2008). Does financial distress risk drive the momentum anomaly? *Financial Management*, *37*(3), 461-484.

Arnott, R. D., Kalesnik, V., & Linnainmaa, J. T. (2023). Factor momentum. *Review of Financial Studies*, *36*(8), 3034-3070.

Asness, C. S., Frazzini, A., & Pedersen, L. H. (2012). Leverage aversion and risk parity. *Financial Analysts Journal*, *68*(1), 47-59.

Bali, T. G., Cakici, N., & Whitelaw, R. F. (2011). Maxing out: Stocks as lotteries and the cross-section of expected returns. *Journal of Financial Economics*, *99*(2), 427-446.

Barberis, N., Jin, L. J., & Wang, B. (2021). Prospect theory and stock market anomalies. *Journal of Finance*, *76*(5), 2639-2687.

Barberis, N., Mukherjee, A., & Wang, B. (2016). Prospect Theory and Stock Returns: An Empirical Test. *Review of Financial Studies*, *29*(11), 3068-3107. https://doi.org/10.1093/rfs/hhw049

Barberis, N., Shleifer, A., & Vishny, R. (1998). A model of investor sentiment. *Journal of Financial Economics*, *49*(3), 307-343.

Benetton, M., & Compiani, G. (2024). Investors' beliefs and cryptocurrency prices. *Review of Asset Pricing Studies*, *14*(2), 197-236.

Berk, J. B., Green, R. C., & Naik, V. (1999). Optimal investment, growth options, and security returns. *Journal of Finance*, *54*(5), 1553-1607.

Biais, B., Bisiere, C., Bouvard, M., Casamatta, C., & Menkveld, A. J. (2023). Equilibrium bitcoin pricing. *Journal of Finance*, *78*(2), 967-1014.

Bolt, W., & Van Oordt, M. R. (2020). On the value of virtual currencies. *Journal of Money, Credit and Banking*, *52*(4), 835-862.

Borri, N., & Shakhnov, K. (2022). The Cross-Section of Cryptocurrency Returns. *Review of Asset Pricing Studies*, *12*(3), 667-705. https://doi.org/10.1093/rapstu/raac007

Chordia, T., & Shivakumar, L. (2002). Momentum, business cycle, and time-varying expected returns. *Journal of Finance*, *57*(2), 985-1019.

Chui, A. C., Titman, S., & Wei, K. J. (2010). Individualism and momentum around the world. *Journal of Finance*, *65*(1), 361-392.

Cohn, J. B., Liu, Z., & Wardlaw, M. I. (2022). Count (and count-like) data in finance. *Journal of Financial Economics*, *146*(2), 529-551.

Cong, L. W., & He, Z. (2019). Blockchain disruption and smart contracts. *Review of Financial Studies*, *32*(5), 1754-1797.

Cong, L. W., Karolyi, G. A., Tang, K., & Zhao, W. (2023). Value premium, network adoption, and factor pricing of crypto assets. *Available at SSRN 3985631*.

Cong, L. W., Li, Y., & Wang, N. (2021). Tokenomics: Dynamic adoption and valuation. *Review of Financial Studies*, *34*(3), 1105-1155.

Cooper, M. J., Gutierrez Jr, R. C., & Hameed, A. (2004). Market states and momentum. *Journal of Finance*, *59*(3), 1345-1365.

Corbet, S., Lucey, B., & Yarovaya, L. (2018). Datestamping the Bitcoin and Ethereum bubbles. *Finance Research Letters*, *26*, 81-88.

Daniel, K., Hirshleifer, D., & Subrahmanyam, A. (1998). Investor psychology and security market under- and overreactions. *Journal of Finance*, *53*(6), 1839-1885.

Daniel, K., & Moskowitz, T. J. (2016). Momentum crashes. *Journal of Financial Economics*, *122*(2), 221-247.

Dow, J., Han, J., & Sangiorgi, F. (2021). Hysteresis in price efficiency and the economics of slow-moving capital. *Review of Financial Studies*, *34*(6), 2857-2909.

Driscoll, J. C., & Kraay, A. C. (1998). Consistent covariance matrix estimation with spatially dependent

panel data. *Review of economics and statistics*, *80*(4), 549-560.
Duffie, D. (2010). Presidential address: Asset price dynamics with slow-moving capital. *Journal of Finance*, *65*(4), 1237-1267.
Duffie, D., Gârleanu, N., & Pedersen, L. H. (2005). Over-the-counter markets. *Econometrica*, *73*(6), 1815-1847.
Duffie, D., Gârleanu, N., & Pedersen, L. H. (2007). Valuation in over-the-counter markets. *Review of Financial Studies*, *20*(6), 1865-1900.
Easley, D., O'Hara, M., & Basu, S. (2019). From mining to markets: The evolution of bitcoin transaction fees. *Journal of Financial Economics*, *134*(1), 91-109.
Ehsani, S., & Linnainmaa, J. T. (2022). Factor momentum and the momentum factor. *The Journal of Finance*, *77*(3), 1877-1919.
Foley, S., Karlsen, J. R., & Putniņš, T. J. (2019). Sex, Drugs, and Bitcoin: How Much Illegal Activity Is Financed through Cryptocurrencies? *The Review of Financial Studies*, *32*(5), 1798-1853. https://doi.org/10.1093/rfs/hhz015
Gabaix, X., & Koijen, R. S. (2021). In search of the origins of financial fluctuations: The inelastic markets hypothesis. *NBER Working Paper Series*.
Gandal, N., & Halaburda, H. (2016). Can we predict the winner in a market with network effects? Competition in cryptocurrency market. *Games*, *7*(3), 16.
Gandal, N., Hamrick, J., Moore, T., & Oberman, T. (2018). Price manipulation in the Bitcoin ecosystem. *Journal of Monetary Economics*, *95*, 86-96.
Garlappi, L., & Yan, H. (2011). Financial distress and the cross-section of equity returns. *Journal of Finance*, *66*(3), 789-822.
Garratt, R., & Wallace, N. (2018). Bitcoin 1, bitcoin 2,....: An experiment in privately issued outside monies. *Economic Inquiry*, *56*(3), 1887-1897.
Ghysels, E., & Nguyen, G. (2019). Price discovery of a speculative asset: Evidence from a bitcoin exchange. *Journal of Risk and Financial Management*, *12*(4), 164.
Greenwood, R., Hanson, S. G., Shleifer, A., & Sørensen, J. A. (2022). Predictable financial crises. *Journal of Finance*, *77*(2), 863-921.
Greenwood, R., Shleifer, A., & You, Y. (2019). Bubbles for fama. *Journal of Financial Economics*, *131*(1), 20-43.
Griffin, J. M., & Shams, A. (2020). Is Bitcoin really untethered? *Journal of Finance*, *75*(4), 1913-1964.
Grinblatt, M., & Han, B. (2005). Prospect theory, mental accounting, and momentum. *Journal of Financial Economics*, *78*(2), 311-339.
Grossman, S. J., & Stiglitz, J. E. (1980). On the impossibility of informationally efficient markets. *American Economic Review*, *70*(3), 393-408.
Grundy, B. D., & Martin, J. S. M. (2001). Understanding the nature of the risks and the source of the rewards to momentum investing. *Review of Financial Studies*, *14*(1), 29-78.
Hautsch, N., Scheuch, C., & Voigt, S. (2024). Building trust takes time: limits to arbitrage for blockchain-based assets. *Review of Finance*, *28*(4), 1345-1381.
Hayes, A. S. (2017). Cryptocurrency value formation: An empirical study leading to a cost of production model for valuing bitcoin. *Telematics and informatics*, *34*(7), 1308-1321.
Hellwig, M. F. (1980). On the aggregation of information in competitive markets. *Journal of Economic Theory*, *22*(3), 477-498.
Hinzen, F. J., John, K., & Saleh, F. (2022). Bitcoin's limited adoption problem. *Journal of Financial Economics*, *144*(2), 347-369.
Hong, H., & Stein, J. C. (1999). A unified theory of underreaction, momentum trading, and overreaction in asset markets. *Journal of Finance*, *54*(6), 2143-2184.
Hubrich, S. (2017). 'Know When to Hodl'Em, Know When to Fodl'Em': An Investigation of Factor Based Investing in the Cryptocurrency Space. *Available at SSRN 3055498*.
Irresberger, F., John, K., Mueller, P., & Saleh, F. (2021). The public blockchain ecosystem: An empirical analysis. *Available at SSRN 3592849*.

Jegadeesh, N., & Titman, S. (1993). Returns to buying winners and selling losers: Implications for stock market efficiency. *Journal of Finance*, *48*(1), 65-91.
John, K., O'Hara, M., & Saleh, F. (2022). Bitcoin and beyond. *Annual Review of Financial Economics*, *14*, 95-115.
Johnson, T. C. (2002). Rational momentum effects. *Journal of Finance*, *57*(2), 585-608.
Kiefer, N. M., & Vogelsang, T. J. (2005). A new asymptotic theory for heteroskedasticity-autocorrelation robust tests. *Econometric Theory*, *21*(6), 1130-1164.
Kim, O., & Verrecchia, R. E. (1994). Market liquidity and volume around earnings announcements. *Journal of Accounting and Economics*, *17*(1-2), 41-67.
Kogan, S., Makarov, I., Niessner, M., & Schoar, A. (2024). Are cryptos different? evidence from retail trading. *Journal of Financial Economics*, *159*, 103897.
Koijen, R. S., & Yogo, M. (2019). A demand system approach to asset pricing. *Journal of Political Economy*, *127*(4), 1475-1515.
Kyle, A. S. (1985). Continuous auctions and insider trading. *Econometrica: Journal of the Econometric Society*, 1315-1335.
Lewellen, J. (2002). Momentum and autocorrelation in stock returns. *Review of Financial Studies*, *15*(2), 533-564.
Li, X., & Wang, C. A. (2017). The technology and economic determinants of cryptocurrency exchange rates: The case of Bitcoin. *Decision support systems*, *95*, 49-60.
Liu, Y., & Tsyvinski, A. (2020). Risks and Returns of Cryptocurrency. *Review of Financial Studies*, *34*(6), 2689-2727. https://doi.org/10.1093/rfs/hhaa113
Liu, Y., Tsyvinski, A., & Wu, X. (2022). Common risk factors in cryptocurrency. *Journal of Finance*, *77*(2), 1133-1177.
Lyandres, E., Palazzo, B., & Rabetti, D. (2022). Initial coin offering (ico) success and post-ico performance. *Management Science*, *68*(12), 8658-8679.
Makarov, I., & Schoar, A. (2020). Trading and arbitrage in cryptocurrency markets. *Journal of Financial Economics*, *135*(2), 293-319.
Moreira, A., & Muir, T. (2017). Volatility-managed portfolios. *Journal of Finance*, *72*(4), 1611-1644.
Rohrbach, J., Suremann, S., & Osterrieder, J. (2019). Momentum and trend following trading strategies for currencies revisited-combining academia and industry. *Available at SSRN 2949379*.
Rubinstein, A., & Wolinsky, A. (1985). Equilibrium in a Market with Sequential Bargaining. *Econometrica*, *53*(5), 1133-1150. https://doi.org/10.2307/1911015
Sagi, J. S., & Seasholes, M. S. (2007). Firm-specific attributes and the cross-section of momentum. *Journal of Financial Economics*, *84*(2), 389-434.
Sockin, M., & Xiong, W. (2023a). Decentralization through Tokenization. *Journal of Finance*, *78*(1), 247-299. https://doi.org/https://doi.org/10.1111/jofi.13192
Sockin, M., & Xiong, W. (2023b). A model of cryptocurrencies. *Management Science*.
Sokolov, K. (2021). Ransomware activity and blockchain congestion. *Journal of Financial Economics*, *141*(2), 771-782.
Stivers, C., & Sun, L. (2010). Cross-sectional return dispersion and time variation in value and momentum premiums. *Journal of Financial and Quantitative Analysis*, *45*(4), 987-1014.
Urquhart, A. (2016). The inefficiency of Bitcoin. *Economics Letters*, *148*, 80-82.
Vayanos, D., & Woolley, P. (2013). An institutional theory of momentum and reversal. *Review of Financial Studies*, *26*(5), 1087-1145.
Zurek, P. (2007). Momentum and long-run risks. *Available at SSRN 972661*.

Table A. Variable Definitions

Variable name	Variable definition
MaxRunup	The maximum price runup experienced by a cryptocurrency. For each cryptocurrency i at the beginning of week t, we first identify its lowest daily closing price ($P_{min,i,t,\tau}$) during a 12-week ranking period (denoted as τ) prior to the week t. We then define price runup as the annualized price change of $P_{min,i,t,\tau}$ with respect to the closing price at the end of week t-1 ($P_{end,i,t-1}$). Mathematically, $MaxRunnup_{i,t} = \left(\frac{P_{end,i,t-1}}{P_{min,i,t,\tau}} - 1\right) * \frac{365}{\#Days}$, where $\#Days$ denotes the number of days between the lowest price date and the end of the ranking period. If the cryptocurrency hits the same lowest price for several different dates, we use the latest date to estimate the maximum runup.
MaxDrawdown	The maximum price drawdown experienced by a cryptocurrency. For each cryptocurrency i at the beginning of week t, we first identify its highest daily closing price ($P_{max,i,t,\tau}$) during a 12-week ranking period (denoted as τ) prior to week t. We then define price runup as the annualized price change of $P_{max,i,t,\tau}$ with respect to the closing price at the end of week t-1 ($P_{end,i,t-1}$). Mathematically, $MaxDrawdown_{i,t} = \left(\frac{P_{end,i,t-1}}{P_{max,i,t,\tau}} - 1\right) * \frac{365}{\#Days}$, where $\#Days$ denotes the number of days between the highest price date and the end of the ranking period. If the cryptocurrency hits the same highest price for several different dates, we use the latest date to estimate the maximum drawdown.
InRank	The degree of inelasticity of each cryptocurrency. At the beginning of week t, we rank the magnitude of *MaxRunup* and *MaxDrawdown* ($\lvert MaxDrawdown_{it} \rvert$), then divide ranks by the number of cross-sectional observations to standardize the magnitude of Runup and Drawdown into the [0, 1], uniformly, denoted as $Rank_{runup,i,t}$ and $Rank_{drawdown,i,t}$. The $Inelasticity_{i,t}$ is: $\left(Rank_{runup,i,t} + Rank_{drawdown,i,t}\right)/2$. We then normalize it into [0, 1], uniformly to calculate *InRank*.
$Inelasticity_{pro}$	The alternative measure of inelasticity, which is constructed as the product of $Rank_{runup,i,t}$ and $Rank_{drawdown,i,t}$, i.e., $\left(Rank_{runup,i,t} \times Rank_{drawdown,i,t}\right)$.
D(Crash)	Cryptocurrency crash. $D(Crash)_{i,t}$ equals one if the cryptocurrency i experiences a price drop, i.e., from $P_{begin,i,t}$ to the minimum price $P_{min,i,t,s}$ in the given holding period (denoted as s) from the beginning of week t, of which the magnitude belongs to the top quintile (i.e., top 20%) of all cryptocurrencies in the given holding period.
D(Bubble)	Cryptocurrency bubble. $D(Bubble)_{i,t}$ equals one if the cryptocurrency i experiences a price rise, i.e., from $P_{begin,i,t}$ to the maximum price $P_{max,i,t,s}$ in the given holding period (denoted as s) from the beginning of week t, of which the magnitude belongs to the top quintile (i.e., top 20%) of all cryptocurrencies in the given holding period.
Ret [-2, -1]	Cumulative returns from the start of week t-2 to the end of week t-1 for each week t, which are calculated as price changes of close prices of week t-3 to week t-1.
Size	The logarithm of the outstanding market capitalization (in dollar) at the beginning of the week t.
lnAmihud	The logarithm of the Amihud illiquidity ratio following Amihud (2002) and Amihud and Noh (2020). The Amihud ratio is defined as the mean value of daily Amihud illiquidity ratio in the past T days prior to the start of week t (day t_0), i.e., ($\frac{1}{T}\sum_{s=t_0-T}^{t_0-1} 10^6 \times \lvert ret_{i,t,s} \rvert / Volumn_{i,t,s}$), where $\lvert ret_{i,t,s} \rvert$ is the absolute value of daily

	return, and $Volumn_{i,t,s}$ is the dollar trading volume for cryptocurrency i at day s, in the forming period prior to week t, respectively.
Turnover	The turnover ratio, measured as the average daily dollar trading volume divided by market capitalization, in the past 12 weeks prior to the start of week *t*.
Ret [-12, -3]	Cumulative returns from the start of week *t*-12 to the end of *t*-3 for each week *t*. We use log returns to deal with the extreme values of long-term returns.
IVOL	The idiosyncratic volatility of cryptocurrencies' daily returns, measured as the standard deviation of residuals in the Cryptocurrency CAPM model over the past 12 weeks prior to the start of each week *t*.
Skewness	The skewness of cryptocurrencies' daily returns over the past 12 weeks prior to the start of each week *t*.
Kurtosis	The kurtosis of cryptocurrencies' daily returns over the past 12 weeks prior to the start of each week *t*.
Google Search	Google search volume. We download the time-series Google Trends of cryptocurrencies' full names worldwide from Google Trend (https://trends.google.com/trends/). Our sample period is from 5 January 2014 to 29 May 2024.
Time	Average Time Between Transactions. The average duration between one transaction block and the next. This is calculated by measuring the total time that it takes in the blockchain to approve one block following the previous block and averaging it daily. The data is from Intotheblock (https://www.intotheblock.com/).
Volume	The average number of transactions for a particular crypto-asset. This data is based on transactions on the blockchain. Therefore, transactions taken within exchanges are not recorded unless they occur on-chain. Following Cong et al., (2023) and Irresberger et al., (2021), the data is from Intotheblock.
Acadr	The average of addresses that made one or more on-chain transactions on a given day. Following Cong et al., (2023) and Irresberger et al., (2021), the data is from Intotheblock.
BA	Total Addresses with Balance. The average of all addresses that currently hold this particular crypto-asset. Following Cong et al., (2023) and Irresberger et al., (2021), the data is from Intotheblock.
BA growth	The weekly logarithmic growth rate of total addresses with balance at week *t*-1, i.e., $log(\frac{Total\ Asset\ with\ Balance_{i,t-1}}{Total\ Asset\ with\ Balance_{i,t-2}})$, following Cong et al., (2023).
Value	The negative of past-52-week returns prior to the start of each week *t*, following Cong et al., (2023).

Table 1. Summary Statistics

This table tabulates the summary statistics of cryptocurrencies. The price and trading volume data (5th Jan 2014-12th May 2024) are from https://coinmarketcap.com/. 4284 cryptocurrencies constitute the whole sample. Panel A reports the number of cryptocurrencies, the mean and median of market capitalization, and the mean and median of daily trading price volume by year. Panel B reports the main weekly variables of our sample, including weekly returns at week *t*, market size (logarithm of market capitalization in dollars) at the beginning of week *t*, logarithmic 12-week average of the Amihud illiquidity ratio and turnover ratio prior to week *t* (lnAmihud), non-annually runups and drawdowns (refer to the Appendix) with 12-week ranking period prior to week *t*, the negative of past 52-week cumulative returns (Value) at the beginning of week *t*, and the log difference of total addresses with balance (BA growth) at the beginning of week *t*. All the continuous variables but returns are winsorized at 1% and 99% percentile. The cryptocurrencies' returns are winsorized at 0.1% and 99.9% percentile.

Panel A: Cryptocurrency Market Summary by Year

Year	Number of Coins	Market Cap (mil)		Volume (thous)	
		Mean	Median	Mean	median
2014	62	326.33	4.93	1512.68	30.63
2015	68	144.65	2.96	1265.84	10.86
2016	131	173.09	3.24	1886.57	18.18
2017	585	535.61	9.01	23010.65	120.32
2018	1,408	414.74	8.97	24085.08	104.57
2019	1,316	274.72	5.63	69831.55	150.54
2020	1,429	371.02	6.99	8908550	278.65
2021	2,344	1358.38	16.35	220478.8	631.58
2022	2,117	955.2	14.12	404592.5	535.93
2023	1,893	937.64	15.57	65386.66	481.58
2024	1,798	1454.54	21.72	106817.6	780.2

Panel B: Summary Statistics in Weekly Sample

	N	#Coins	mean	std	p25	median	p75	skew	kurtosis
Ret (fraction)	393,191	4,284	0.01	0.27	-0.85	-0.11	-0.01	0.07	3.53
Size (log dollar)	393,191	4,284	16.60	2.03	13.82	15.01	16.24	17.77	27.97
lnAmihud	393,188	4,284	-3.97	3.73	-12.70	-6.45	-4.27	-1.86	6.05
Turnover(fraction)	393,191	4,284	0.12	0.22	0.00	0.01	0.04	0.13	1.46
IVOL	391,430	4,284	0.09	0.11	0.00	0.04	0.06	0.10	0.84
Runup (fraction)	393,191	4,284	1.18	2.98	0.00	0.10	0.32	0.90	22.48
Drawdown (fraction)	393,191	4,284	-0.38	0.24	-0.90	-0.56	-0.37	-0.19	0.00
BA growth	82,807	514	0.01	0.03	0.00	0.00	0.01	3.80	18.46
Value (fraction)	371,729	4,036	-2.38	10.81	-0.68	0.28	0.69	-6.03	39.20

Table 2. The Determinants of Financial Inelasticity

This table explores the determinants of financial Inelasticity with a non-overlapping sample (sampling every twelve weeks) by conducting the following regression:

$$InRank_{i,q} = a + \beta_1 \times Time_{i,q} + \beta_2 \times \#Transaction_{i,q} + \gamma \times Time_{i,q} \times \#Transaction_{i,q} + C \times M_{i,q} + v_i + u_q + \varepsilon_{i,q},$$

where the main variables of interest are the average time between transactions (Time) and the number of transactions (#Transaction). We also control for the number of active addresses (ActAdr) and the number of addresses with balance (BA). These variables are constructed as the logarithm of the average values over the past 12 weeks (one quarter). Columns (1) through (3) include coin fixed effects (v_i) and time fixed effects (u_q). Column (4) further incorporates Blockchain×Time fixed effects. T-statistics based on standard errors clustered at the cryptocurrency level are in parentheses. *, **, and *** represent statistical significance at 10%, 5% and 1%, respectively.

	(1)	(2)	(3)	(4)
Dep. Var =		InRank		
Time	0.040***	0.035***	0.031***	0.041***
	(4.49)	(4.13)	(3.54)	(4.32)
#Transaction	0.059***	0.035***	0.061***	0.089***
	(5.92)	(3.45)	(4.09)	(5.18)
Time × #Transaction		0.005***	0.003***	0.003***
		(5.29)	(3.48)	(2.66)
ActAdr			-0.018	-0.034**
			(-1.38)	(-2.30)
BA			-0.029***	-0.022***
			(-4.07)	(-3.20)
Observations	7,407	7,397	6,933	6,933
Adj R^2	0.205	0.210	0.214	0.214
Coin FE	YES	YES	YES	YES
Time FE	YES	YES	YES	NO
Blockchain × Time FE	NO	NO	NO	YES

Table 3. Performance by Double-sorted Runups and Drawdowns

This table presents the portfolio performance across runup and drawdown double-sorted groups. At the beginning of each week *t*, we divide the cryptocurrencies into the top 30%, middle 40%, and bottom 30% groups, according to their magnitude of *MaxRunup* and *MaxDrawdown* (Ranking period=12 weeks, prior to week *t*), respectively and independently. Panel A and B present the portfolio performance and the return spreads between each group and the mid/mid group, respectively. The value-weighted portfolios are weekly rebalanced and held for one week. Raw returns, Crypto-CAPM adjusted returns, Crypto-three-factor model (CMKT, CSIZE, CMOM) adjusted returns, and Crypto-five-factor model ($CMKT_{C5}$, $CSMB_{C5}$, $CVAL_{C5}$, $CNET_{C5}$, and CMOM) adjusted returns are reported. *T*-statistics adjusted by Newey-West heteroskedasticity in parentheses. *, **, and *** denote significance at the 10%, 5%, and 1% level, respectively.

Panel A: Portfolio Performance

	Excess Return			**CAPM Alpha**		
	Drawdown			Drawdown		
MaxRunup	1(Low)	2	3(High)	1(Low)	2	3(High)
1 (Low)	0.008	0.011	-0.003	0.000	0.000	-0.014
	(1.58)	(1.56)	(-0.38)	(-0.09)	(-0.07)	(-2.46)
2	0.023	0.011	0.011	0.011	-0.001	-0.001
	(3.10)	(1.63)	(1.26)	(2.50)	(-0.32)	(-0.14)
3(High)	0.011	0.003	-0.015	-0.001	-0.010	-0.026
	(1.22)	(0.35)	(-1.73)	(-0.11)	(-1.55)	(-4.21)

	Three Factor Alpha			**Five Factor Alpha**		
	Drawdown			Drawdown		
MaxRunup	1(Low)	2	3(High)	1(Low)	2	3(High)
1 (Low)	0.000	0.004	-0.012	-0.006	-0.003	-0.019
	(0.15)	(0.72)	(-2.15)	(-1.93)	(-0.78)	(-3.35)
2	0.011	-0.002	0.003	0.004	-0.009	-0.009
	(2.46)	(-0.63)	(0.40)	(1.10)	(-2.17)	(-2.14)
3(High)	-0.005	-0.009	-0.025	-0.014	-0.014	-0.030
	(-0.72)	(-1.57)	(-4.46)	(-2.35)	(-2.29)	(-5.25)

Panel B: Portfolio Performance (Diff. from mid/mid group)

	Excess Return			**CAPM Alpha**		
	Drawdown			Drawdown		
MaxRunup	1(Low)	2	3(High)	1(Low)	2	3(High)
1 (Low)	-0.003	0.000	-0.015	0.000	0.001	-0.014
	(-0.71)	(-0.00)	(-2.73)	(0.09)	(0.17)	(-2.46)
2	0.012	0	0.000	0.012	0	0.000
	(2.65)		(-0.06)	(2.76)		(-0.04)
3(High)	-0.001	-0.008	-0.026	0.000	-0.009	-0.024
	(-0.10)	(-1.39)	(-3.75)	(0.04)	(-1.68)	(-3.71)

	Three Factor Alpha			**Five Factor Alpha**		
	Drawdown			Drawdown		
MaxRunup	1(Low)	2	3(High)	1(Low)	2	3(High)
1 (Low)	0.002	0.006	-0.011	0.003	0.006	-0.011
	(0.48)	(1.11)	(-2.05)	(0.66)	(1.04)	(-1.98)
2	0.013	0	0.004	0.013	0	0.000
	(2.88)		(0.61)	(2.69)		(-0.00)
3(High)	-0.003	-0.008	-0.023	-0.005	-0.006	-0.021
	(-0.39)	(-1.46)	(-3.84)	(-0.74)	(-0.99)	(-3.35)

Table 4. InRank-sorted Crypto Portfolio

At the beginning of each week t, we sort cryptocurrencies into five groups by their Inelasticity (ranking period=12 weeks, prior to week t). *Panel* A presents excess returns, Crypto-CAPM adjusted alphas, Crypto-three-factor model (CMKT, CSMB, CMOM) adjusted alphas, and Crypto-five-factor model ($CMKT_{C5}$, $CSMB_{C5}$, $CVAL_{C5}$, $CNET_{C5}$, and CMOM) adjusted alphas of the value-weighted portfolios with h-week (h=1, 4, 8) holding period from the start of week t. EMI denotes the differences between the Elastic group (group 1) and the Inelastic group (group 5). Following Jegadeesh and Titman (1993), at each given week T, a series of groups selected at the current week and at the previous h-1 weeks are held, where h denotes the holding periods. Then we revise the weights on $1/h$ of these groups to get the average portfolio returns. *Panel* B presents the median of cryptocurrencies' characteristics in each group, including Size (log market value), lnAmihud (logarithm of Amihud illiquidity ratio), Turnover ratio, IVOL (idiosyncratic volatility), Skewness, and Kurtosis. T-statistics adjusted by Newey-West heteroskedasticity with 5 lags are in parentheses. *, **, and *** denote significance at the 10%, 5%, and 1% level, respectively.

Panel A: The Portfolio Performance of Groups Sorted by Inelasticity

	1 (Elastic)	**2**	**3**	**4**	**5 (Inelastic)**	**EMI (Elastic-minus-Inelastic)**		
	h = 1 week						h=4week	h=8week
Excess Return	0.013	0.016	0.006	0.009	-0.011	0.025***	0.019***	0.023***
	(2.55)	(2.22)	(0.87)	(1.12)	(-1.42)	(4.71)	(3.17)	(4.35)
CAPM Alpha	0.004	0.005	-0.005	-0.003	-0.023	0.026***	0.022***	0.026***
	(1.58)	(1.05)	(-1.13)	(-0.72)	(-4.30)	(5.27)	(4.02)	(5.28)
Three Factor	0.004	0.005	-0.005	-0.002	-0.021	0.026***	0.021***	0.025***
	(1.63)	(1.10)	(-0.99)	(-0.34)	(-4.41)	(5.53)	(3.94)	(5.10)
Five Factor	-0.001	-0.002	-0.010	-0.009	-0.026	0.024***	0.019***	0.023***
	(-0.31)	(-0.58)	(-2.71)	(-2.48)	(-5.30)	(5.38)	(3.43)	(4.64)

Panel B: The Portfolios' Characteristics.

	1 (Elastic)	**2**	**3**	**4**	**5 (Inelastic)**	**EMI (Elastic-minus-Inelastic)**
Size	16.87	16.39	16.14	15.98	15.77	1.11***
lnAmihud	-4.34	-3.4	-2.71	-2.44	-1.37	-2.97***
Turnover	0.09	0.08	0.08	0.08	0.09	0.00
IVOL	0.05	0.07	0.1	0.11	0.18	-0.13***
Skewness	0.6	0.88	1.18	1.37	2.01	-1.41***
Kurtosis	5.76	6.04	7.58	8.45	11.85	-6.09***

Table 5. Predicting Crypto Returns by Inelasticity

This table investigates the predictability of Inelasticity on weekly returns using Fama-MacBeth regressions:

$$Ret_{i,t} = \alpha_t + \beta \times InRank_{i,t-1} + \gamma \times X_{i,t-1} + \varepsilon_{i,t},$$

where InRank is the cross-section rank of Inelasticity, which is uniformly standardized between [0, 1]. Columns (4)-(6) replace InRank with a dummy variable indicating the top 20% inelastic cryptocurrencies (Inelasticity Dummy). Control variables include Ret [a, b] (cumulative returns from the start of week *t+a* to the end of week *t+b*), Size (logarithm of market value at the beginning of week *t*), lnAmihud (logarithm of average past 12-week Amihud illiquidity ratios prior to week *t*), Turnover (average past 12-week turnover ratios prior to week *t*), IVOL (idiosyncratic volatility based on Crypto-CAPM in the past 12 weeks prior to week *t*), Skewness and Kurtosis. The bottom rows present time-series averaged adjusted R^2, sample periods, and observations. *T*-statistics adjusted by Newey-West heteroskedasticity with 5 lags are in parentheses. *, **, and *** denote significance at the 10%, 5%, and 1% level, respectively.

	(1)	(2)	(3)	(4)	(5)	(6)
Dep. Var =			Ret			
InRank	-0.016***	-0.015***	-0.055***			
	(-3.77)	(-2.98)	(-8.55)			
Inelasticity Dummy				-0.012***	-0.010***	-0.025***
				(-3.76)	(-3.14)	(-7.25)
Ret [-2, -1]		-0.007	-0.019**		-0.006	-0.018***
		(-0.92)	(-2.55)		(-0.90)	(-2.76)
Size		0.000	-0.001		0.001	0.000
		(0.25)	(-0.90)		(0.52)	(-0.30)
lnAmihud		0.001	-0.003***		0.001	-0.003**
		(1.44)	(-2.75)		(1.59)	(-2.48)
Turnover		0.141	-0.128		0.135	0.209
		(0.95)	(-0.58)		(0.91)	(0.44)
Ret [-12,-3]			-0.009***			-0.010***
			(-3.08)			(-3.27)
IVOL			0.213***			0.156***
			(3.48)			(3.09)
Skewness			0.037***			0.037***
			(8.49)			(9.21)
Kurtosis			-0.003***			-0.003***
			(-6.58)			(-6.80)
Adj R^2	0.004	0.044	0.093	0.007	0.049	0.095
Weeks	540	540	540	540	540	540
obs	388,955	388,953	388,948	388,955	388,953	388,948

Table 6. Predicting Crashes by Inelasticity

This table investigates the predictability of Inelasticity on crashes:

$$D_{i,t+h-1}(Crash) = \alpha_0 + \beta_1 \times InRank_{i,t-1} + c \times X_{i,t-1} + \varepsilon_{i,t+h-1},$$

where $D_{i,t+h-1}(Crash)$ equals one if a cryptocurrency i experiences a crash during the h-week (h=1, 4, and 8) holding period after week t. A crash is characterized by large price changes from the start of week t to its trough, which fall within the top 20% of the magnitude in the cross-section. InRank is the standardized cross-section rank of Inelasticity. Columns (2), (4) and (6) replace InRank with a dummy variable indicating the top 20% inelastic cryptocurrencies (Inelasticity Dummy). Panel A presents the results of prediction on crashes using the linear model, and Panel B reports the results of average semi-elasticities using the panel logit model. InRank is the cross-section rank of Inelasticity, which is uniformly standardized between [0, 1]. Inelasticity Dummy equals one if the cryptocurrency belongs to the highest quintile (i.e., top 20%) of Inelasticity. Control variables include Ret [-12, -1] (logarithm of cumulative returns from the start of week t-12 to the end of week t-1), Size (logarithm of market value at the beginning of week t), lnAmihud (logarithm of average past 12-week Amihud illiquidity ratios prior to the start of week t), Turnover (average past 12-week turnover ratios prior to the start of week t), IVOL (idiosyncratic volatility based on Crypto-CAPM in the past 12 weeks prior to the start of week t), Skewness, and Kurtosis. u_i denotes the coin-fixed effects. *T*-statistics are shown in parentheses. The p-values in Panel A are based on Driscoll and Kraay (1998) standard errors with (2, 6, 12) lags for h=1, 4, 8, respectively, and corrected according to Kiefer and Vogelsang (2005). Standard errors in Panel B are clustered at the cryptocurrency level. *, **, and *** denote significance at the 10%, 5%, and 1% level, respectively

Panel A: Predicting Crashes						
	(1)	(2)	(3)	(4)	(5)	(6)
	Holding Period=1 Week		Holding Period=4 Weeks		Holding Period=8 Weeks	
InRank	0.152***		0.128***		0.098***	
	(32.33)		(15.32)		(9.12)	
Inelasticity Dummy		0.087***		0.077***		0.063***
		(27.34)		(14.44)		(9.82)
Size	0.041***	0.041***	0.036***	0.036***	0.038***	0.038***
	(29.97)	(29.24)	(18.51)	(18.24)	(12.67)	(12.55)
lnAmihud	0.042***	0.043***	0.027***	0.027***	0.021***	0.022***
	(58.53)	(58.91)	(27.59)	(28.04)	(18.48)	(18.53)
Turnover	0.127***	0.133***	0.080***	0.085***	0.057***	0.061***
	(18.82)	(19.71)	(10.26)	(10.70)	(5.11)	(5.41)
Ret [-12, -1]	0.019***	0.019***	0.024***	0.024***	0.027***	0.027***
	(8.61)	(8.73)	(6.95)	(7.12)	(6.24)	(6.38)
IVOL	0.289***	0.312***	0.321***	0.337***	0.264***	0.274***
	(14.06)	(15.09)	(9.71)	(10.11)	(6.46)	(6.81)
Skewness	-0.015***	-0.013***	-0.014***	-0.013***	-0.012***	-0.011***
	(-8.31)	(-7.71)	(-6.64)	(-6.40)	(-5.17)	(-5.02)
Kurtosis	0.001***	0.001**	0.001*	0.000	0.001	0.000
	(2.67)	(2.47)	(1.71)	(1.60)	(1.58)	(1.53)
Observations	385,994	385,994	381,294	381,294	374,890	374,890
Number of Coins	4,265	4,265	4,232	4,232	4,171	4,171
Coin FE	YES	YES	YES	YES	YES	YES

Panel B: Predicting Crashes Using Panel Logit Model						
	(1)	(2)	(3)	(4)	(5)	(6)
	Holding Period=1 Week		Holding Period=4 Weeks		Holding Period=8 Weeks	
lnRank	0.898***		0.780***		0.631***	
	(50.64)		(35.10)		(25.06)	
Inelasticity Dummy		0.401***		0.366***		0.316***
		(39.81)		(30.79)		(24.49)
Size	0.226***	0.224***	0.212***	0.211***	0.236***	0.235***
	(26.10)	(25.15)	(20.51)	(19.95)	(18.62)	(18.31)
lnAmihud	0.222***	0.224***	0.145***	0.148***	0.120***	0.122***
	(47.12)	(46.66)	(29.64)	(29.60)	(20.66)	(20.80)
Turnover	0.706***	0.738***	0.497***	0.526***	0.389***	0.412***
	(20.26)	(20.65)	(11.41)	(11.90)	(6.74)	(7.09)
Ret [-12, -1]	0.089***	0.094***	0.109***	0.113***	0.128***	0.130***
	(12.58)	(12.97)	(12.64)	(12.86)	(12.24)	(12.34)
IVOL	0.938***	1.122***	1.090***	1.238***	0.893***	0.999***
	(11.87)	(13.71)	(11.62)	(12.99)	(8.02)	(8.91)
Skewness	-0.077***	-0.065***	-0.072***	-0.062***	-0.058***	-0.051***
	(-12.27)	(-10.00)	(-8.99)	(-7.60)	(-5.80)	(-4.99)
Kurtosis	0.005***	0.004***	0.004***	0.003**	0.003**	0.003*
	(5.36)	(4.15)	(3.32)	(2.56)	(2.39)	(1.94)
Observations	381,212	381,212	371,276	371,276	359,593	359,593
Number of Coins	3,938	3,938	3,747	3,747	3,528	3,528
Coin FE	YES	YES	YES	YES	YES	YES

Table 7. Momentum and InRank Double-sorted Portfolios

This table presents the performance of portfolios double-sorted by two-week Momentum and Inelasticity. At the beginning of each week t, cryptocurrencies are divided into three groups: the bottom 30%, medium 40%, and top 30%, based on their past two-week returns and InRank (12-week ranking period) independently. These portfolios are held for one week, and if a portfolio has no cryptocurrencies, the value is left missing. The EMI Average denotes the average performance of the EMI strategy within each momentum group. To construct the *ElasticWinner-Minus-InelasticLoser* (*EWIL*) Strategy, at the beginning of each week t, we first sort cryptocurrencies into the bottom 30%, medium 40%, and top 30% groups according to their InRanks. Within each group, we further divide cryptocurrencies into the bottom 30%, medium 40%, and top 30% groups according to their past two-week returns. The EWIL Strategy is to long Elastic-Winner portfolios and short Inelastic-Loser portfolios. Value-weighted raw returns and alphas adjusted by Crypto-CAPM, Crypto-three-factor model (CMKT, CSMB, CMOM), and Crypto-five-factor model ($CMKT_{C5}$, $CSMB_{C5}$, $CVAL_{C5}$, $CNET_{C5}$, and CMOM) are presented in each panel. T-statistics adjusted by Newey-West heteroskedasticity with 5 lags are in parentheses. *, **, and *** represent statistical significance at 10%, 5% and 1%, respectively.

		InRank						
	Momentum	1 (Elastic)	2	3 (Inelastic)	EMI	EMI Average	Momentum Average	EWIL
Excess Return	1 (Loser)	0.002	0.001	-0.007	0.008			
		(0.40)	(0.12)	(-1.02)	(1.43)			
	2	0.012	0.007	0.004	0.010			
		(2.07)	(0.96)	(0.38)	(1.56)			
	3 (Winner)	0.023	0.016	-0.003	0.027***			
		(3.24)	(1.80)	(-0.35)	(4.08)			
	WML	0.021***	0.015**	0.004		0.013***	0.014***	0.034***
		(4.11)	(2.41)	(0.62)		(3.34)	(3.30)	(5.99)
CAPM Alpha	1 (Loser)	-0.008	-0.010	-0.018	0.009			
		(-2.09)	(-2.38)	(-3.62)	(1.49)			
	2	0.002	-0.005	-0.009	0.012**			
		(0.65)	(-1.35)	(-1.37)	(2.07)			
	3 (Winner)	0.012	0.005	-0.014	0.027***			
		(2.62)	(0.76)	(-2.32)	(4.14)			
	WML	0.021***	0.014**	0.004		0.015***	0.013***	0.034***
		(4.24)	(2.43)	(0.63)		(3.77)	(3.49)	(6.29)
Three Factor	1 (Loser)	-0.005	-0.007	-0.013	0.006			
		(-1.32)	(-1.76)	(-2.48)	(1.05)			
	2	0.003	-0.005	-0.007	0.011**			
		(1.03)	(-1.30)	(-1.10)	(1.99)			
	3 (Winner)	0.009	0.002	-0.016	0.026***			
		(2.16)	(0.38)	(-2.72)	(4.01)			
	WML	0.016***	0.009*	-0.003		0.014***	0.007**	0.033***
		(3.28)	(1.65)	(-0.45)		(3.58)	(2.08)	(6.01)
Five Factor	1 (Loser)	-0.010	-0.016	-0.024	0.014**			
		(-2.48)	(-4.55)	(-5.31)	(2.57)			
	2	-0.001	-0.013	-0.010	0.009			
		(-0.44)	(-3.10)	(-1.67)	(1.48)			
	3 (Winner)	0.002	-0.001	-0.021	0.022***			
		(0.43)	(-0.21)	(-3.87)	(3.63)			
	WML	0.011**	0.015***	0.003		0.012***	0.009***	0.032***
		(2.41)	(2.68)	(0.53)		(2.84)	(2.66)	(6.18)

Table 8. Down-Market Betas for Enhanced Momentum Strategies

In this table, we follow Daniel and Moskowitz (2016) to estimate the down-market betas of the momentum portfolio:

$$\tilde{R}_{WML,t} = (\alpha_0 + \alpha_B * I_{B,t-1}) + (\beta_0 + I_{B,t-1}(\beta_B + \tilde{I}_{U,t}\beta_{B,U})) * \tilde{R}_{Mkt,t} + \tilde{\epsilon}_t,$$

where $\tilde{R}_{WML,t}$ is the 2-week Winners-minus-Losers (WML) return in week t, $\tilde{R}_{Mkt,t}$ represents the value-weighted index of all the cryptocurrencies in week t, $I_{B,t-1}$ denotes an ex-ante bear market indicator that equals one if the cumulative VW index return in the past 4 weeks is negative, and is zero otherwise, $\tilde{I}_{U,t}$ is a contemporaneous, i.e., not ex-ante, up-market indicator variable that equals one if the excess VW index return is greater than the risk-free rate in week t, and is zero otherwise. Given that the duration of crashes in the cryptocurrency market is not as long as the equity market, the down-market is estimated as a negative market return in the 4 weeks prior to the holding period. At the beginning of each week t, we divide the cryptocurrencies into three groups (30% Losers, 40% Mid, and 30% Winners) by their two-week cumulative returns to construct the WML strategy. To construct the *ElasticWinner-Minus-InelasticLoser* (EWIL), we first sort the cryptocurrencies into three groups (30% Elastic, 40% Mid, and 30% Inelastic) according to their Inelasticity. Within each Inelasticity-ranked group, we further divide the cryptocurrencies into three groups (30% Losers, 40% Mid, and 30% Winners) by their two-week cumulative returns. The EWIL is to long the Elastic-Winner group and short the Inelastic-Loser group. We apply the same tests to the EMI strategy (Elastic-minus-Inelastic) and the EWIL.*T*-statistics adjusted by Newey-West heteroskedasticity with 5 lags are reported in parentheses*, **, and *** indicate significance levels of 10%, 5%, and 1%, respectively.

Coef.	Dep. Var = Indep. Var	R_{WML} (1)	EMI (2)	EWIL (3)	R_{WML} (4)	EMI (5)	EWIL (6)
$\tilde{\beta}_0$	$\tilde{R}_{Mkt,t}$	-0.018	-0.159***	-0.010	-0.216**	-0.212***	-0.300***
		(-0.29)	(-2.65)	(-0.11)	(-2.42)	(-3.33)	(-3.01)
$\tilde{\alpha}_B$	$I_{B,t-1}$				0.021	-0.016	0.001
					(1.44)	(-0.98)	(0.07)
$\tilde{\beta}_B$	$I_{B,t-1}\tilde{R}_{Mkt,t}$				0.455**	-0.105	0.270
					(2.20)	(-0.80)	(1.62)
$\tilde{\beta}_{B,U}$	$I_{B,t-1}\tilde{I}_{U,t}\tilde{R}_{Mi}$				-0.088	0.365	0.533**
					(-0.31)	(1.14)	(2.10)
$\tilde{\alpha}_0$		0.022***	0.026***	0.035***	0.009	0.027***	0.019**
		(4.27)	(5.19)	(6.53)	(1.14)	(4.00)	(2.54)

Table 9. DiD Regressions: ICO-induced Inelasticity

This table presents the results of DiD regressions investigating the effects of ICOs on Inelasticity and network congestion, and the corresponding dynamic treatment effects:

$$InRank_{i,t} \ \ or \ CAR_{i,t} = a + \beta \times Treat_{i,t} + \gamma \times X_{i,t} + u_{i \times Event} + v_{t \times Event} + \varepsilon_{i,t},$$

$$InRank_{i,t} \ \ or \ CAR_{i,t} = a + \sum_{j=-3, j \neq -1}^{4} \beta_j \times ETH_i \times I\{t = \tau + j\} + \gamma \times X_{i,t} + u_{i \times Event} + v_{t \times Event} + \varepsilon_{i,t},$$

where the dependent variables include the InRank and cumulative returns. InRank is the cross-section rank of Inelasticity, which is uniformly standardized between [0, 1]. The event window is from τ-3 week to τ+4 week, where τ denotes the start week of ICOs. CAR is the buy-and-hold cumulative cryptocurrency returns from τ-3. $Treat_{i,t} = ETH_i \times After_{i,t}$, equals one if the cryptocurrency i is based on Ethereum and treated after the start date of ICO events. $I\{t = \tau + j\}$ are indicators that equal one if the week is j week after the ICO events. Control variables include Ret [-13, -2], Ret [-2, -1], Size, lnAmihud, Turnover, IVOL, Skewness, Kurtosis, BA growth, and value. We control for the crypto-event $u_{i \times Event}$ and week-event fixed effects $v_{t \times Event}$. Panel A presents the results on InRank and cumulative returns, and Panel B presents the results on average time between transactions (Time), abnormal transactions (AbVolume, the log difference of the number of transactions in the current week and average number of transactions in 12 weeks before ICO events), and Google Search Trend (Google Search). We conduct Fixed-effects Poisson regressions on Time and Google Search in Panel B. T-statistics based on standard errors clustered at blockchain-event and week levels are shown in parentheses. *, **, and *** represent statistical significance at 10%, 5% and 1%, respectively.

Panel A: Inelasticity and Cumulative Returns around ICO Events				
	(1)	(2)	(3)	(4)
	InRank		Cumulative Returns	
Treat	0.076***		-0.208**	
	(3.40)		(-2.57)	
$ETH_i \times I\{t = \tau - 3\}$		-0.040		0.044
		(-1.31)		(0.70)
$ETH_i \times I\{t = \tau - 2\}$		0.007		-0.021
		(0.32)		(-0.52)
$ETH_i \times I\{t = \tau\}$		0.045**		-0.055
		(2.04)		(-1.14)
$ETH_i \times I\{t = \tau + 1\}$		0.044**		-0.136**
		(2.07)		(-2.23)
$ETH_i \times I\{t = \tau + 2\}$		0.049**		-0.296**
		(2.25)		(-2.54)
$ETH_i \times I\{t = \tau + 3\}$		0.074**		-0.243***
		(2.18)		(-2.70)
$ETH_i \times I\{t = \tau + 4\}$		0.118***		-0.282**
		(2.97)		(-2.61)
Controls	YES	YES	YES	YES
Coin-Event FE	YES	YES	YES	YES
Week-Event FE	YES	YES	YES	YES
Observations	48,408	48,408	49,212	49,212
R^2	0.749	0.750	0.845	0.846

Panel B: Average time, Abnormal Transactions, and Google Search around ICO Events			
	(1)	(2)	(3)
	Time	AbVolume	Google Search
Treat	0.282**	-0.147***	0.245***
	(2.31)	(-2.73)	(3.47)
Ret [-2, -1]	-0.239**	0.156*	0.084*
	(-2.08)	(1.67)	(1.66)
Size	-0.582***	0.582***	0.149
	(-3.25)	(4.66)	(0.96)
lnAmihud	-0.099	-0.011	0.143*
	(-0.60)	(-0.13)	(1.68)
Turnover	1.304	0.194	0.870*
	(0.88)	(0.23)	(1.65)
Ret [-12,-3]	-0.017**	-0.003	-0.006
	(-2.35)	(-0.35)	(-0.76)
IVOL	-17.162***	9.481**	-0.623
	(-2.88)	(2.31)	(-0.16)
Skewness	0.107	-0.104	0.056
	(1.10)	(-1.58)	(0.60)
Kurtosis	0.010	0.014	-0.006
	(0.51)	(1.25)	(-0.40)
BA growth	-5.905*	1.089	-0.781
	(-1.72)	(0.57)	(-1.03)
Value	-0.002	0.004**	-0.003**
	(-0.78)	(2.53)	(-2.38)
Coin-Event FE	YES	YES	YES
Week-Event FE	YES	YES	YES
Observations	45,768	48,462	48,248
(Pseudo) R^2	0.991	0.841	0.649

Table 10.Robustness Checks on Return Prediction

In this table, we conduct Fama-MacBeth predictive regressions on returns for robustness check. Column (1) includes a dummy variable RunupFirst, which equals one if the $Date_{min}$ is prior to $Date_{max}$, and its interaction term with InRank. Columns (2) to (4) examine the predictability in the sample of the largest cryptocurrencies (top 500 in terms of market cap) and of the cryptos issued before or after EOS (July 1st, 2017). Columns (5) to (6) present the results in subsamples of coins and tokens, respectively, according to CoinGecko and Internet search. Column (6) investigates an alternative measure for Inelasticity, $Inelasticity_{pro}$, which is constructed by the product of $Rank_{runup,i,t}$ and $Rank_{drawdown,i,t}$. Column (8) excludes stablecoins. We require at least 24 observations in the cross-section. T-statistics adjusted by Newey-West heteroskedasticity with 5 lags are in parentheses. *, **, and *** denote significance at the 10%, 5%, and 1% level, respectively.

					Subsample by Crypto Types		Alternative Measure	Exclude Stablecoin
	Sequence	Top 500	Before EOS	After EOS	Coins	Tokens	InelasPro	
	(1)	(2)	(3)	(4)	(5)	(6)	(7)	(8)
InRank	**-0.088***	**-0.044***	**-0.051***	**-0.048***	**-0.047***	**-0.047***	**-0.042***	**-0.055***
	(-5.95)	**(-7.96)**	**(-7.04)**	**(-12.62)**	**(-7.51)**	**(-8.80)**	**(-8.23)**	**(-8.48)**
×RunupFirst	0.027							
	(1.14)							
Ret [-2, -1]	-0.024***	-0.008	-0.041***	-0.027***	-0.017**	-0.029***	-0.014***	-0.020***
	(-3.10)	(-1.54)	(-4.51)	(-8.83)	(-2.24)	(-7.73)	(-2.74)	(-2.63)
Size	-0.001	-0.002	-0.001	-0.002**	-0.004**	-0.001	-0.001	-0.001
	(-0.32)	(-1.37)	(-0.36)	(-2.37)	(-2.04)	(-0.74)	(-1.01)	(-0.95)
lnAmihud	-0.003*	-0.003***	-0.003**	-0.003***	-0.006***	-0.002***	-0.003***	-0.004***
	(-1.95)	(-2.95)	(-2.45)	(-4.74)	(-3.77)	(-3.13)	(-2.69)	(-2.84)
Turnover	-0.061	-0.222	-0.126	-0.040***	-0.422**	-0.023	-0.215	-0.187
	(-0.28)	(-1.11)	(-0.57)	(-2.85)	(-2.06)	(-1.35)	(-1.09)	(-0.80)
Ret [-12, -3]	-0.012***	-0.008***	-0.018***	-0.014***	-0.012***	-0.014***	-0.011***	-0.010***
	(-2.93)	(-2.73)	(-4.20)	(-7.82)	(-3.37)	(-6.00)	(-3.87)	(-3.20)
IVOL	0.210***	0.122***	0.252***	0.157***	0.246***	0.124***	0.135***	0.217***
	(3.45)	(2.59)	(3.65)	(7.15)	(4.99)	(4.88)	(3.35)	(3.58)
Skewness	0.037***	0.035***	0.034***	0.038***	0.044***	0.041***	0.037***	0.039***
	(8.22)	(8.57)	(7.54)	(9.62)	(8.67)	(10.16)	(9.16)	(8.43)
Kurtosis	-0.003***	-0.003***	-0.003***	-0.004***	-0.005***	-0.004***	-0.003***	-0.004***
	(-6.14)	(-6.68)	(-5.71)	(-7.69)	(-7.73)	(-7.44)	(-7.19)	(-6.86)
First-RU	0.004							
	(0.24)							
Observations	388,948	182,898	67,640	379,687	90,229	295,371	388,275	381,492
Adj R^2	0.098	0.111	0.160	0.062	0.129	0.076	0.088	0.094

Figure 1. Performance of Crypto Portfolios with Low-mid-High InRanks

This figure displays the performance of crypto portfolios with high-mid-low InRanks and the time-series performance of the EMI (Elastic-minus-Inelastic) strategy. At the beginning of each week *t*, the cryptocurrencies are sorted into five groups according to their InRank. Each group is value-weighted, held for one week, and rebalanced weekly. The Middle group's return is the average of returns of group 2 to group 4. This figure shows the time-series performance of Elastic (blue solid line), Mid (red long dash line), Inelastic groups (green dash line), and EMI strategy (black bold solid line) (log 10) in our sample period from Jan. 2014 to May. 2024.

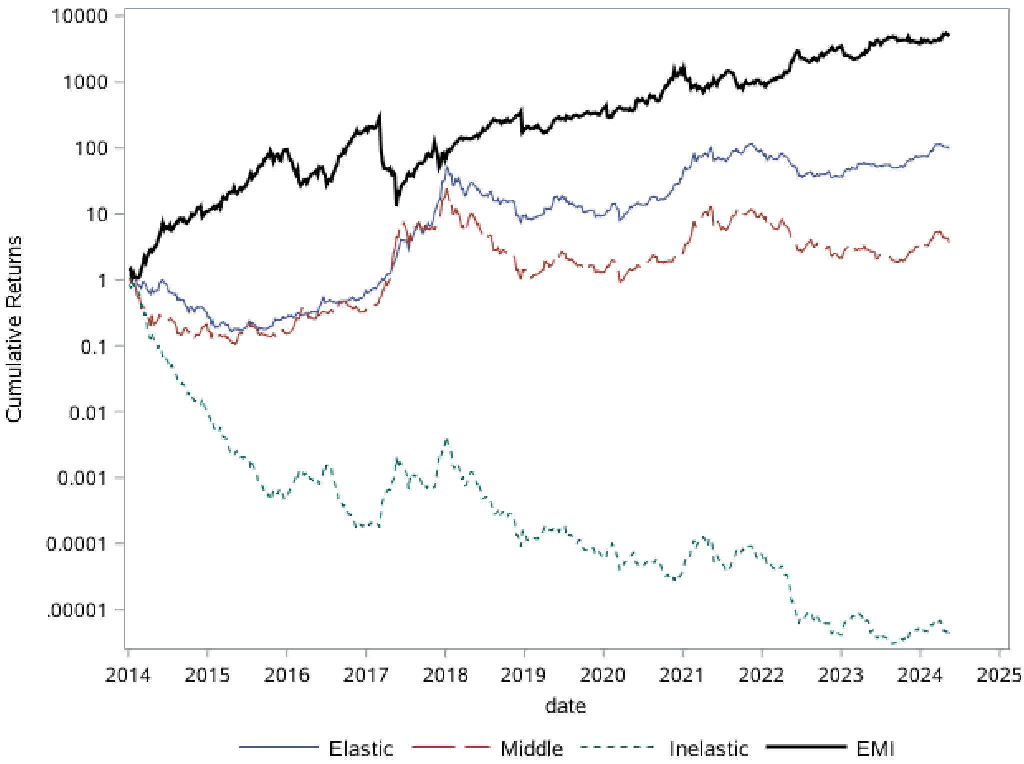

Figure 2. ElasticWinner-Minus-InelasticLoser (EWIL) Strategy

This figure displays the performance of the Momentum strategy (WML) and the *ElasticWinner-Minus-InelasticLoser* strategy, with 90% confidence intervals. To construct the Momentum Strategy, at the beginning of each week *t*, we split the cryptocurrencies into three groups (bottom 30%, medium 40%, and top 30%) based on their past two-week returns. The Momentum strategy is to long the winners (top 30%) and short the losers (bottom 30%). To construct the EWIL strategy, we first divide the cryptocurrencies into three groups (bottom 30%, medium 40%, and top 30%) based on InRanks (namely 'E,' 'M_elastic,' and 'I,' respectively). Within each Inelasticity-ranked group, we sort the cryptocurrencies into three groups (bottom 30%, medium 40%, and top 30%) based on their past two-week returns (namely 'L,' 'M_mom,' and 'W,' respectively). The EWIL Strategy is to long cryptocurrencies in the 'EW' group and short cryptocurrencies in the 'IL' group. All portfolios are value-weighted. We estimate Crypto-CAPM betas using weekly returns from week $t-28$ to $t-2$ (approximately half a year) and then compute the cumulative abnormal returns (CAR) for the 52-week holding period adjusted by the Crypto-CAPM model.

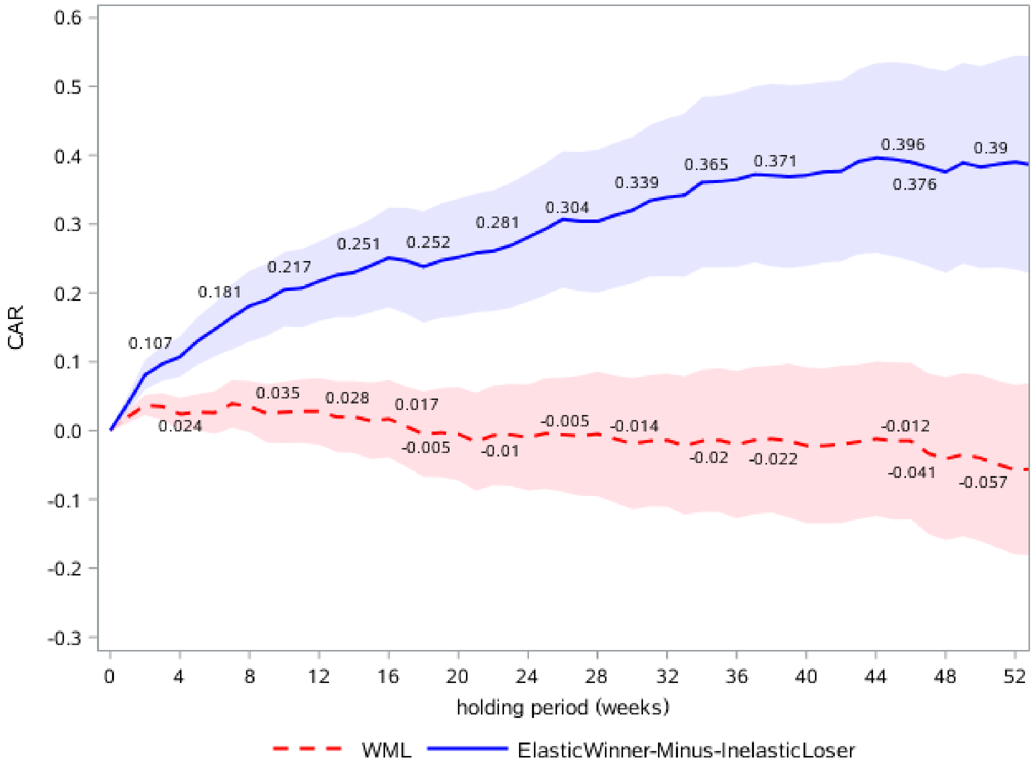

Figure 3. Dynamic Treatment Effect

This figure illustrates the dynamic treatment effects on InRank (Panel A) and Cumulative Returns (Panel B) during the [-3 weeks, +4 weeks] window around events. The figures display the coefficients associated with a 90% confidence interval of the dynamic treatment effect with controls.

Panel A: *InRank*

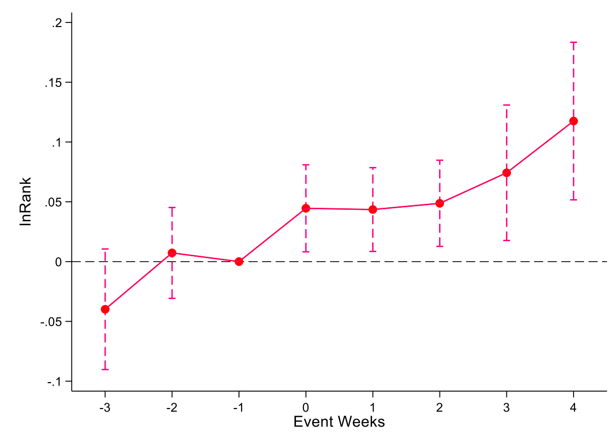

Panel B: *Cumulative Returns*

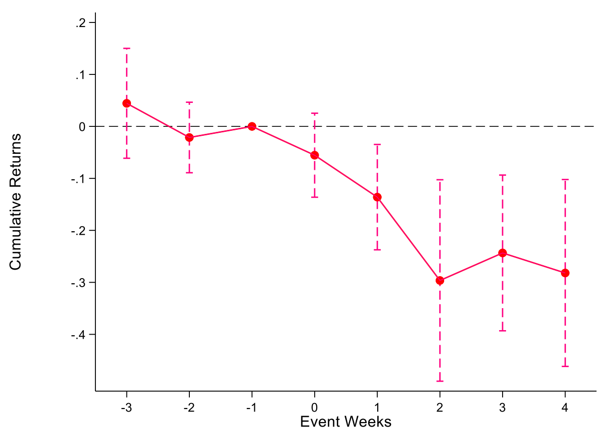

Internet Appendix

Predictive Crypto Crashes

Table A1. Supplementary Summary Statistics

This table presents summary statistics for other variables supplementary to Table 1. Panel A reports the summary statistics of factors, i.e., the Crypto-three-factor model ($CMKT$, $CSMB$, $CMOM$) and the Crypto-five-factor model ($CMKT_{C5}$, $CSMB_{C5}$, $CVAL_{C5}$, $CNET_{C5}$, and $CMOM$). Panel B reports summary statistics of variables on network and Google search, including the 12-week logarithmic average time between transactions (Time), logarithmic average transaction numbers (Volume), logarithmic average number of total addresses with balance (BA), logarithmic average number of active addresses (ActAdr), logarithmic number of Google Search. All continuous variables are winsorized at 1% and 99% percentile.

Panel A: Crypto Factors

	Period	mean	std	p25	median	p75	skew	kurtosis
$CMKT$	5th Jan, 2014 – 12th May, 2024	0.013	0.113	-0.037	0.005	0.060	1.687	17.263
$CSMB$	5th Jan, 2014 –12th May, 2024	0.007	0.085	-0.029	0.006	0.037	1.129	7.532
$CMOM$	5th Jan, 2014 –12th May, 2024	0.011	0.106	-0.039	0.004	0.048	0.752	8.230
$CMKT_{C5}$	8th June, 2014 –12th May, 2024	0.019	0.144	-0.043	0.009	0.070	1.861	10.237
$CSMB_{C5}$	8th June, 2014–12th May, 2024	0.027	0.146	-0.024	0.013	0.059	4.847	62.466
$CVAL_{C5}$	8th June, 2014–12th May, 2024	0.014	0.109	-0.026	0.012	0.052	-0.637	11.698
$CNET_{C5}$	8th June, 2014–12th May, 2024	0.003	0.151	-0.034	0.010	0.052	-2.019	19.080

Panel B: Network and Google Search

	N	#Coins	mean	std	p25	median	p75	skew	kurtosis
Time	7,389	531	7.792	2.434	6.204	7.645	9.338	0.224	3.387
Volume	7,377	531	4.466	2.487	2.842	4.332	5.711	1.015	5.212
ActAdr	7,406	532	4.309	2.266	2.820	4.050	5.328	1.368	6.114
BA	7,602	534	9.636	1.958	8.537	9.430	10.44	0.760	7.336
Google Search	7,191	523	32.41	40.93	5.083	19.17	49.50	5.601	89.13

Table A2. Characteristics of Double-sorted Portfolios across Runup and Drawdown.

This table presents other characteristics of double-sorted portfolios by *MaxRunup* and *MaxDrawdown* in Table 3. The characteristics include the cross-section factions of cryptocurrencies falling into each group, average idiosyncratic volatility, kurtosis and skewness, size (logarithm of the outstanding market capitalization), turnover ratio, lnAmihud (logarithm of Amihud illiquidity ratio), Ret [-12, -1] (logarithm of past 12-week returns prior to week *t*), and the magnitude of runups and drawdowns in each group.

		Characteristics	MaxDrawdown			Characteristics	MaxDrawdown		
			1	2	3		1	2	3
	1	fraction	0.10	0.14	0.07	Turnover	0.10	0.08	0.09
MaxRunup	2		0.12	0.17	0.11		0.08	0.08	0.09
	3		0.08	0.10	0.12		0.07	0.08	0.08
	1	IVOL	0.05	0.07	0.10	lnAmihud	-5.11	-3.51	-2.90
MaxRunup	2		0.07	0.09	0.11		-4.04	-3.38	-2.92
	3		0.14	0.15	0.20		-2.73	-2.56	-2.26
	1	Kurtosis	7.41	7.78	11.02	Ret[-12, -1]	-0.11	-0.33	-0.38
MaxRunup	2		7.34	8.77	10.77		0.09	-0.10	0.06
	3		11.92	12.29	16.57		0.61	0.26	0.79
	1	Skew	0.67	1.01	1.48	MaxRunup	1.91	2.05	2.29
MaxRunup	2		0.97	1.23	1.59		7.02	7.07	7.32
	3		1.80	1.85	2.49		32.85	29.10	38.50
	1	SIZE	17.12	16.20	15.88	MaxDrawdown	1.25	2.76	6.17
MaxRunup	2		16.82	16.21	15.95		1.31	2.82	6.76
	3		16.21	15.92	15.82		1.10	2.92	8.40

Table A3. Runup- and Drawdown-sorted Portfolios with Different Holding Periods

This table presents the portfolio performance across runup and drawdown double-sorted groups with different holding periods (h = 4, 8 weeks). At the beginning of each week t, we divide the cryptocurrencies into the top 30%, middle 40%, and bottom 30% groups, according to their magnitude of runup and drawdown (Ranking period=12 weeks, prior to week t), respectively and independently. Panel A, B, C, and D present the portfolio performance and the return spreads between each group and the mid/mid group, respectively. The value-weighted portfolios are weekly rebalanced. Following Jegadeesh and Titman (1993), at each given week T, a series of groups selected at the current week as well as at the previous h-1 weeks are held, where h denotes the holding periods. Then we revise the weights on 1/h of these groups to get the average portfolio returns. Raw returns, Crypto-CAPM, Crypto-three-factor model, and Crypto-five-factor model adjusted returns are reported. T-statistics adjusted by Newey-West heteroskedasticity are in parentheses. *, **, and *** denote significance at the 10%, 5%, and 1% level, respectively.

Panel A: Portfolio Performance (Holding Period = 4 Weeks)

	Excess Return			**CAPM Alpha**			**Three Factor Alpha**			**Five Factor Alpha**		
	MaxDrawdown			MaxDrawdown			MaxDrawdown			MaxDrawdown		
MaxRunup	1(Low)	2	3(High)	1(Low)	2	3(High)	1(Low)	2	3(High)	1(Low)	2	3(High)
1 (Low)	0.010	0.012	0.008	0.001	0.001	-0.005	0.002	0.002	-0.002	-0.004	-0.006	-0.011
	(1.85)	(1.73)	(1.07)	(0.46)	(0.18)	(-1.00)	(0.68)	(0.53)	(-0.32)	(-1.40)	(-1.92)	(-2.80)
2	0.023	0.012	0.005	0.011	0.000	-0.006	0.010	0.001	-0.004	0.002	-0.006	-0.014
	(2.98)	(1.74)	(0.77)	(2.40)	(0.00)	(-1.52)	(2.23)	(0.16)	(-0.91)	(0.77)	(-1.92)	(-4.45)
3(High)	0.009	0.007	-0.004	-0.002	-0.005	-0.016	-0.003	-0.005	-0.015	-0.011	-0.010	-0.021
	(1.22)	(0.92)	(-0.52)	(-0.39)	(-1.00)	(-3.03)	(-0.73)	(-1.12)	(-2.95)	(-2.77)	(-2.30)	(-4.81)

Panel B: Portfolio Performance (Diff. from mid/mid group) (Holding Period = 4 Weeks)

	Excess Return			**CAPM Alpha**			**Three Factor Alpha**			**Five Factor Alpha**		
	MaxDrawdown			MaxDrawdown			MaxDrawdown			MaxDrawdown		
MaxRunup	1(Low)	2	3(High)	1(Low)	2	3(High)	1(Low)	2	3(High)	1(Low)	2	3(High)
1 (Low)	-0.003	0.000	-0.005	0.001	0.000	-0.005	0.001	0.001	-0.003	0.002	0.000	-0.006
	(-0.67)	(-0.13)	(-1.34)	(0.21)	(0.09)	(-1.54)	(0.26)	(0.38)	(-0.79)	(0.56)	(-0.01)	(-1.61)
2	0.011	0	-0.007	0.011	0	-0.007	0.010	0	-0.005	0.008	0	-0.008
	(2.84)		(-2.05)	(3.08)		(-2.23)	(2.60)		(-1.58)	(2.91)		(-2.71)
3(High)	-0.003	-0.004	-0.016	-0.002	-0.005	-0.016	-0.004	-0.006	-0.015	-0.005	-0.005	-0.015
	(-0.69)	(-1.21)	(-3.57)	(-0.50)	(-1.53)	(-3.62)	(-0.99)	(-1.81)	(-3.58)	(-1.20)	(-1.28)	(-3.34)

Panel C: Portfolio Performance (Holding Period = 8 Weeks)

	Excess Return			**CAPM Alpha**			**Three Factor Alpha**			**Five Factor Alpha**		
	MaxDrawdown			MaxDrawdown			MaxDrawdown			MaxDrawdown		
MaxRunup	1(Low)	2	3(High)	1(Low)	2	3(High)	1(Low)	2	3(High)	1(Low)	2	3(High)
1 (Low)	0.013	0.014	0.011	0.004	0.002	-0.002	0.005	0.003	0.001	-0.002	-0.006	-0.009
	(2.46)	(1.96)	(1.44)	(1.40)	(0.42)	(-0.33)	(1.47)	(0.65)	(0.13)	(-0.74)	(-2.09)	(-2.06)
2	0.023	0.014	0.010	0.007	0.002	-0.002	0.007	0.003	0.000	0.003	-0.004	-0.009
	(2.90)	(2.12)	(1.43)	(1.87)	(0.60)	(-0.54)	(1.89)	(0.78)	(-0.13)	(0.76)	(-1.26)	(-2.97)
3(High)	0.012	0.009	-0.002	-0.003	-0.003	-0.014	-0.003	-0.003	-0.013	-0.004	-0.010	-0.018
	(1.57)	(1.19)	(-0.22)	(-0.77)	(-0.82)	(-2.95)	(-0.71)	(-0.86)	(-2.85)	(-0.79)	(-2.77)	(-4.55)

Panel D: Portfolio Performance (Diff. from mid/mid group) (Holding Period = 8 Weeks)

	Excess Return			**CAPM Alpha**			**Three Factor Alpha**			**Five Factor Alpha**		
	MaxDrawdown			MaxDrawdown			MaxDrawdown			MaxDrawdown		
MaxRunup	1(Low)	2	3(High)	1(Low)	2	3(High)	1(Low)	2	3(High)	1(Low)	2	3(High)
1 (Low)	-0.001	-0.001	-0.004	0.002	-0.001	-0.004	0.002	-0.001	-0.003	0.002	-0.002	-0.005
	(-0.37)	(-0.52)	(-1.05)	(0.51)	(-0.41)	(-1.13)	(0.53)	(-0.33)	(-0.64)	(0.65)	(-1.17)	(-1.52)
2	0.008	0	-0.005	0.005	0	-0.005	0.004	0	-0.004	0.007	0	-0.005
	(1.99)		(-1.89)	(1.69)		(-2.15)	(1.33)		(-1.78)	(1.67)		(-2.20)
3(High)	-0.003	-0.006	-0.016	-0.006	-0.006	-0.017	-0.006	-0.007	-0.016	-0.001	-0.007	-0.015
	(-0.60)	(-1.81)	(-3.98)	(-1.63)	(-2.17)	(-4.20)	(-1.75)	(-2.49)	(-4.14)	(-0.13)	(-2.38)	(-3.81)

Table A4. Predicting Crashes Using Different Specifications

This table investigates the predictability of Inelasticity on crashes using alternative specifications. Specifically, Panel A presents the results of the linear prediction model with two-way fixed effects (columns (1), (3), and (5)), and the linear prediction model controlling the level of large runups and large drawdowns (columns (2), (4), and (6)). Panel B presents the robustness check on predicting net crashes. We define the binary outcome of a cryptocurrency crash (bubble) if the cryptocurrency experiences a large price change (from the start of week *t* to its trough or peak), which belongs to the bottom (top) 20% in the *h*-week holding period. Net Crash refers to the cryptocurrency experiencing a crash but not a bubble. The results with *h*=1, 4, and 8-week holding periods are tabulated, respectively. Inelasticity Dummy equals one if the cryptocurrency belongs to the highest quintile (i.e., top 20%) of Inelasticity. DRUs and DDDs are dummy variables which equal one if the cryptocurrency belongs to the top 20% on the magnitude of Runups and Drawdowns in the ranking periods. The other control variables include Ret [-12, -1] (logarithm of cumulative returns from the start of week *t*-12 to the end of week *t*-1), Size (logarithm of market value at the beginning of week *t*), lnAmihud (logarithm of average past 12-week Amihud illiquidity ratios prior to the start of week *t*), Turnover (average past 12-week turnover ratios prior to the start of week *t*), IVOL (idiosyncratic volatility based on the Crypto-CAPM in the past 12 weeks prior to the start of week *t*), Skewness and Kurtosis. We use the method of Kiefer and Vogelsang (2005) corrected *p*-values with (2, 6, 12) lags for *h*=1, 4, 8. *, **, and *** denote significance at the 10%, 5%, and 1% level, respectively.

Panel A: Predicting Crashes with Alternative Specifications						
	D(Crash)					
	Holding Period = 1 Week		Holding Period = 4 Weeks		Holding Period = 8 Weeks	
	(1)	(2)	(3)	(4)	(5)	(6)
Inelasticity Dummy	0.077***	0.023***	0.064***	0.019***	0.048***	0.014***
	(24.11)	(7.93)	(13.39)	(4.85)	(9.22)	(3.61)
DRUs		0.145***		0.124***		0.102***
		(42.26)		(22.22)		(14.27)
DDDs		0.021***		0.027***		0.024***
		(7.45)		(7.73)		(5.98)
Size	0.055***	0.040***	0.056***	0.035***	0.061***	0.037***
	(34.88)	(30.67)	(20.38)	(18.62)	(15.50)	(12.70)
lnAmihud	0.044***	0.041***	0.028***	0.026***	0.022***	0.021***
	(68.40)	(60.40)	(30.58)	(27.91)	(17.92)	(18.50)
Turnover	0.144***	0.128***	0.098***	0.081***	0.075***	0.057***
	(20.58)	(20.18)	(10.85)	(11.15)	(5.76)	(5.41)
Ret [-12, -1]	0.030***	0.011***	0.037***	0.016***	0.041***	0.021***
	(11.04)	(5.48)	(9.20)	(5.28)	(9.94)	(5.19)
IVOL	0.367***	0.218***	0.415***	0.256***	0.368***	0.206***
	(19.40)	(10.75)	(14.57)	(7.66)	(11.87)	(5.06)
Skewness	-0.011***	-0.015***	-0.008***	-0.014***	-0.005**	-0.012***
	(-4.78)	(-8.70)	(-3.38)	(-7.18)	(-1.97)	(-5.63)
Kurtosis	0.000	0.001***	-0.000	0.001**	-0.001**	0.001**
	(0.02)	(3.29)	(-1.31)	(2.16)	(-2.19)	(1.96)
Observations	385,994	385,994	381,294	381,294	374,890	374,890
Coin FE	YES	YES	YES	YES	YES	YES
Time FE	YES	NO	YES	NO	YES	NO

Panel B: Predicting Net Crashes						
	D (Net Crash)					
	Holding Period = 1 Week		Holding Period = 4 Week		Holding Period = 8 Week	
	(1)	(2)	(3)	(4)	(5)	(6)
lnRank	0.139***		0.117***		0.092***	
	(31.74)		(14.38)		(8.69)	
Inelasticity Dummy		0.075***		0.067***		0.057***
		(26.43)		(13.49)		(9.40)
Size	0.037***	0.038***	0.035***	0.035***	0.038***	0.038***
	(28.03)	(27.40)	(18.30)	(18.05)	(12.43)	(12.32)
lnAmihud	0.033***	0.034***	0.020***	0.021***	0.016***	0.016***
	(47.80)	(48.37)	(20.37)	(20.77)	(13.21)	(13.31)
Turnover	0.109***	0.115***	0.069***	0.074***	0.051***	0.055***
	(16.17)	(17.06)	(9.19)	(9.61)	(4.75)	(5.05)
Ret [-12, -1]	0.022***	0.023***	0.027***	0.027***	0.029***	0.029***
	(11.15)	(11.13)	(8.86)	(9.03)	(7.37)	(7.50)
IVOL	0.083***	0.107***	0.113***	0.131***	0.094**	0.104***
	(4.66)	(5.93)	(3.91)	(4.47)	(2.57)	(2.91)
Skewness	-0.016***	-0.014***	-0.014***	-0.013***	-0.012***	-0.011***
	(-8.91)	(-8.40)	(-6.57)	(-6.35)	(-5.13)	(-5.01)
Kurtosis	0.001***	0.001***	0.001***	0.001***	0.001***	0.001***
	(5.41)	(5.31)	(4.01)	(4.00)	(3.53)	(3.58)
Observations	385,994	385,994	381,294	381,294	374,890	374,890
Number of Coins	4,265	4,265	4,232	4,232	4,171	4,171
Coin FE	YES	YES	YES	YES	YES	YES

Table A5. Predicting Crashes with a Non-overlapping Sample

This table presents the results of InRank's predictability on crashes with non-overlapping ranking-period observations (i.e., sampling every 12 weeks):

$$D(Crash)_{i,t\ to\ t+h-1} = \alpha + \beta \times InRank_{i,t-1} + \gamma \times X_{i,t-1} + u_i + \varepsilon_{i,t+1\ to\ t+h-1},$$

where $D(Crash)_{i,t\ to\ t+h-1}$ equals one if a cryptocurrency i experiences a crash or a net crash during the h-week holding period after week t. A crash or bubble is characterized by large price changes from the start of week t to its trough or peak, which fall within the bottom or top 20% in the cross section. Net crash refers to the cryptocurrency experiencing a crash but not a bubble. Here we show the results with h=4 and 8-week holding periods, respectively. InRank is the cross-section rank of Inelasticity, which is uniformly standardized between [0, 1]. Columns (2), (4), (6), and (8) replace InRank with a dummy variable indicating the top 20% inelastic cryptocurrencies (Inelasticity Dummy). $X_{i,t-1}$ is a vector of control variables, which includes Ret [-12, -1] (logarithm of cumulative returns from the start of week t-12 to the beginning of week t), Size (logarithm of market value at the beginning of week t), lnAmihud (logarithm of average past 12-week Amihud illiquidity ratios prior to the start of week t), Turnover (average past 12-week turnover ratios prior to the start of week t), IVOL (idiosyncratic volatility based on Crypto-CAPM in the past 12 weeks prior to the start of week t), Skewness and Kurtosis. u_i is the individual fixed effect. T-statistics based on standard errors clustered at the cryptocurrency level are shown in parentheses. *, ** and *** denote significance at the 10%, 5% and 1% level, respectively.

	(1)	(2)	(3)	(4)	(5)	(6)	(7)	(8)
	Holding Period = 4 Weeks				Holding Period = 8 Weeks			
	D(Crash)		D(Net Crash)		D(Crash)		D(Net Crash)	
InRank	0.112***		0.102***		0.089***		0.084***	
	(12.28)		(11.52)		(9.87)		(9.68)	
Inelasticity Dummy		0.072***		0.061***		0.061***		0.054***
		(10.11)		(8.78)		(8.76)		(7.96)
Size	0.035***	0.035***	0.034***	0.034***	0.037***	0.037***	0.037***	0.037***
	(10.95)	(10.85)	(10.82)	(10.72)	(12.16)	(12.10)	(12.33)	(12.27)
lnAmihud	0.025***	0.025***	0.018***	0.018***	0.022***	0.022***	0.017***	0.018***
	(13.71)	(13.84)	(10.47)	(10.60)	(12.63)	(12.73)	(10.07)	(10.17)
Turnover	0.080***	0.083***	0.063***	0.066***	0.068***	0.070***	0.058***	0.060***
	(5.59)	(5.80)	(4.48)	(4.70)	(4.65)	(4.77)	(3.98)	(4.13)
Ret [-12, -1]	0.021***	0.021***	0.025***	0.025***	0.026***	0.025***	0.025***	0.025***
	(6.09)	(5.94)	(7.40)	(7.29)	(7.44)	(7.27)	(7.55)	(7.42)
IVOL	0.378***	0.389***	0.167***	0.180***	0.284***	0.288***	0.129***	0.137***
	(9.04)	(9.33)	(4.45)	(4.81)	(7.09)	(7.26)	(3.36)	(3.59)
Skewness	-0.020***	-0.019***	-0.019***	-0.018***	-0.014***	-0.013***	-0.013***	-0.012***
	(-7.08)	(-6.78)	(-6.99)	(-6.69)	(-5.15)	(-4.94)	(-4.94)	(-4.70)
Kurtosis	0.001**	0.001**	0.002***	0.002***	0.001	0.001	0.001***	0.001***
	(2.32)	(2.29)	(4.14)	(4.10)	(1.34)	(1.33)	(2.73)	(2.71)
Observations	30,960	30,960	30,960	30,960	30,960	30,960	30,960	30,960
Coin FE	YES	YES	YES	YES	YES	YES	YES	YES

Table A6. Robustness Check on Independent Sorted EWIL

This table presents the robustness check on the performance of the independent sorted ElasticWinner-Minus-InelasticLoser (IEWIL) strategy. At the beginning of each week t, cryptocurrencies are divided into the bottom 30%, medium 40%, and top 30% groups according to their past two-week returns and InRank (12-week ranking period) independently and are held for one week. If no cryptocurrency exists in a group, we leave the value missing. The IEWIL is to long elastic-winner portfolios and short inelastic-loser portfolios. Value-weighted raw returns and alphas adjusted by Crypto-CAPM, Crypto-three-factor model (CMKT, CSMB, CMOM), and Crypto-five-factor model ($CMKT_{C5}$, $CSMB_{C5}$, $CVAL_{C5}$, $CNET_{C5}$, and CMOM) are shown in the table. T-statistics adjusted by Newey-West heteroskedasticity with 5 lags are in parentheses. *, **, and *** represent statistical significance at 10%, 5%, and 1%, respectively.

	Excess Return	CAPM Alpha	Three Factor Alpha	Five Factor Alpha
IEWIL	0.029***	0.029***	0.021***	0.022***
	(4.34)	(4.53)	(3.41)	(3.65)

Table A7. Size, Amihud Ratio, and InRank Double-sorted Portfolios

This table presents the value-weighted average excess return to portfolio double sorted, independently on size or Amihud illiquidity ratio and Inelasticity. At the beginning of each week *t*, we independently double-sorted the cryptocurrencies into nine groups on their market value or Amihud illiquidity ratio and InRanks. Cryptocurrencies are divided into the bottom 30%, medium 40%, and top 30% groups according to size or amihud illiquidity ratio and Inelasticity. Within each size-ranked or Amihud illiquidity ratio-ranked group, we construct EMI as the return spread between the Elastic group and the Inelastic group. We also present the average excess returns and alphas on Elastic-minus-Inelastic (EMI) strategy in each size or Amihud group. Raw returns and alphas adjusted by the Crypto-CAPM, the Crypto-three-factor model, and the Crypto-five-factor model are shown in each panel. *T*-statistics based on Newey-West standard errors with four lags are in parentheses. *, **, and *** represent statistical significance at 10%, 5% and 1%, respectively.

Size	1 (Elastic)	2 (Middle)	3 (Inelastic)	EMI	EMI Average
			Excess Return		
1(Small)	0.024	0.016	0.013	0.009*	
	(2.83)	(1.91)	(1.50)	(1.95)	
2	0.012	0.016	0.000	0.013***	
	(1.97)	(2.11)	(-0.03)	(2.69)	
3 (Big)	0.014	0.011	-0.003	0.017***	
	(2.61)	(1.52)	(-0.41)	(3.12)	
3-1	-0.010	-0.006	-0.017***		0.011***
	(-1.56)	(-0.94)	(-2.65)		(3.91)
			CAPM Alpha		
1(Small)	0.013	0.005	0.002	0.010**	
	(2.16)	(0.90)	(0.29)	(2.15)	
2	0.002	0.004	-0.012	0.014***	
	(0.63)	(0.89)	(-2.03)	(3.06)	
3 (Big)	0.004	-0.001	-0.016	0.019***	
	(1.73)	(-0.23)	(-2.96)	(3.79)	
3-1	-0.009	-0.007	-0.018***		0.013***
	(-1.64)	(-1.06)	(-3.01)		(4.68)
			Three Factor Alpha		
1(Small)	0.010	0.002	0.000	0.010**	
	(2.00)	(0.47)	(-0.04)	(2.11)	
2	0.003	0.005	-0.011	0.014***	
	(0.82)	(0.99)	(-2.03)	(3.30)	
3 (Big)	0.004	-0.002	-0.014	0.018***	
	(1.84)	(-0.44)	(-2.83)	(3.77)	
3-1	-0.006	-0.004	-0.014***		0.013***
	(-1.24)	(-0.78)	(-2.60)		(4.75)
			Five Factor Alpha		
1(Small)	-0.001	-0.010	-0.010	0.009*	
	(-0.19)	(-2.04)	(-1.67)	(1.77)	
2	-0.005	-0.008	-0.021	0.016***	
	(-1.44)	(-2.05)	(-4.20)	(3.72)	
3 (Big)	-0.001	-0.006	-0.017	0.015***	
	(-0.20)	(-1.88)	(-3.53)	(3.15)	
3-1	0.001	0.004	-0.007		0.010***
	(0.15)	(0.77)	(-1.05)		(3.51)

Amihud	1 (Elastic)	2 (Middle)	3 (Inelastic)	EMI	EMI Average
			Excess Return		
1(Liquidity)	0.014	0.011	0.002	-0.011**	
	(2.62)	(1.58)	(0.22)	(-1.97)	
2	0.016	0.013	-0.008	-0.023***	
	(2.09)	(1.78)	(-0.93)	(-4.29)	
3 (Illiquidity)	0.020	0.004	-0.008	-0.027***	
	(2.26)	(0.43)	(-0.88)	(-3.09)	
3-1	0.005	-0.007	-0.007		0.020***
	(0.82)	(-0.97)	(-0.90)		(4.33)
			CAPM Alpha		
1(Liquidity)	0.014	0.011	0.002	-0.011**	
	(2.62)	(1.58)	(0.22)	(-1.97)	
2	0.016	0.013	-0.008	-0.023***	
	(2.09)	(1.78)	(-0.93)	(-4.29)	
3 (Illiquidity)	0.020	0.004	-0.008	-0.027***	
	(2.26)	(0.43)	(-0.88)	(-3.09)	
3-1	0.005	-0.007	-0.007		0.020***
	(0.82)	(-0.97)	(-0.90)		(4.33)
			Three Factor Alpha		
1(Liquidity)	0.014	0.011	0.002	-0.011**	
	(2.62)	(1.58)	(0.22)	(-1.97)	
2	0.016	0.013	-0.008	-0.023***	
	(2.09)	(1.78)	(-0.93)	(-4.29)	
3 (Illiquidity)	0.020	0.004	-0.008	-0.027***	
	(2.26)	(0.43)	(-0.88)	(-3.09)	
3-1	0.005	-0.007	-0.007		0.020***
	(0.82)	(-0.97)	(-0.90)		(4.33)
			Five Factor Alpha		
1(Liquidity)	0.004	-0.001	-0.009	-0.013***	
	(1.84)	(-0.23)	(-1.88)	(-2.70)	
2	0.007	0.001	-0.020	-0.026***	
	(1.29)	(0.17)	(-4.15)	(-5.15)	
3 (Illiquidity)	0.006	-0.009	-0.019	-0.025***	
	(1.14)	(-1.40)	(-2.69)	(-2.98)	
3-1	0.002	-0.008	-0.007		0.020***
	(0.37)	(-1.08)	(-1.00)		(4.73)

Table A8. Return Predictability Controlling for Alternative Economic Channels

This table investigates the predictability of Inelasticity on weekly returns controlling for alternative economic channels using Fama-MacBeth regressions:

$$Ret_{i,t} = \alpha_t + \beta \times InRank_{i,t-1} + \gamma \times X_{i,t-1} + \varepsilon_{i,t},$$

where InRank is the cross-section rank of Inelasticity, which is uniformly standardized between [0, 1]. Columns (4) to (6) replace InRank with a dummy variable indicating the top 20% inelastic cryptocurrencies (Inelasticity Dummy). In addition to Ret [a, b], Size, lnAmihud, Turnover, IVOL, Skewness, and Kurtosis, we further control for additional variables, such as BA growth (the weekly growth rate of total addresses with balance at week t-1) and value (the negative of past-52-week return prior to week t) in columns (1) and (4), MAX (the maximum daily returns in week t-1, proxy for lottery demand) and T-K value (proxy for prospect theory preference) in columns (2) and (5), and an indicator for POW consensus in columns (3) and (6). The bottom rows present the time-series averaged adjusted R^2, sample periods, and observations. *T*-statistics adjusted by Newey-West heteroskedasticity with 5 lags are in parentheses. *, **, and *** denote significance at the 10%, 5%, and 1% level, respectively.

	(1)	(2)	(3)	(4)	(5)	(6)
InRank	-0.061***	-0.055***	-0.056***			
	(-4.71)	(-8.47)	(-5.23)			
Inelasticity Dummy				-0.025***	-0.020***	-0.024***
				(-5.56)	(-4.43)	(-5.43)
Ret [-2, -1]	-0.047***	-0.013*	-0.044***	-0.051***	-0.016**	-0.036***
	(-4.30)	(-1.83)	(-3.81)	(-3.33)	(-2.28)	(-4.23)
Size	0.002	-0.001	0.002	0.002	0.000	0.002
	(0.66)	(-0.76)	(0.73)	(0.92)	(0.02)	(0.89)
lnAmihud	-0.002	-0.003***	-0.002*	0.000	-0.002*	-0.002
	(-1.55)	(-2.61)	(-1.73)	(-0.06)	(-1.96)	(-1.07)
Turnover	-0.090**	0.067	-0.071*	-0.003	0.180	-0.028
	(-2.02)	(0.16)	(-1.75)	(-0.05)	(0.42)	(-0.75)
Ret [-12,-3]	-0.027***	-0.004	-0.025***	-0.020***	-0.007*	-0.022***
	(-4.55)	(-1.02)	(-4.96)	(-4.90)	(-1.70)	(-6.04)
IVOL	0.511***	0.232***	0.490***	0.227**	0.144**	0.276***
	(2.82)	(3.53)	(2.95)	(2.57)	(2.25)	(4.23)
Skewness	0.032***	0.038***	0.030***	0.029***	0.037***	0.030***
	(8.70)	(8.42)	(7.85)	(7.07)	(8.51)	(7.57)
Kurtosis	-0.002**	-0.004***	-0.002***	-0.002	-0.003***	-0.002***
	(-2.15)	(-6.32)	(-4.01)	(-1.25)	(-6.14)	(-3.81)
BA growth	0.063*			0.066**		
	(1.91)			(2.00)		
Value	0.000			0.000		
	(-0.25)			(-0.25)		
MaxRet		-0.002*			-0.002*	
		(-1.76)			(-1.83)	
TK Value		-0.127			-0.099	
		(-1.24)			(-0.90)	
POW			0.004			0.004
			(0.67)			(0.80)
Adj R^2	0.112	0.112	0.106	0.103	0.115	0.102
Weeks	353	540	353	353	540	353
Observations	94,367	380,621	94,367	94,367	380,621	94,367

Table A9. Volatility-Managed Factor Alphas

This table presents the results of volatility-managed factor alphas. Panel A presents the excess returns of CMKT, the EMI (the Elastic-minus-Inelastic) strategy, the WML (the two-week momentum) strategy, the EWIL (ElasticWinner-Minus-InelasticLoser), and corresponding volatility-managed factors. The volatility-managed factor f^{σ}, scales by the factors' inverse realized variance in the proceeding 12 weeks $f^{\sigma} = \frac{c}{RV_{t-1}^2} f_t$. Panel B presents the results of univariate regressions of managed factors f^{σ} on unmanaged factors f, where Alpha (α) are the intercepts of the regressions. The sample period of managed factors is from April 2014 to May 2024, as a duration of 12 weeks is required for the calculation of the realized variance. T-statistics adjusted by Newey-West heteroskedasticity with 5 lags are in parentheses. *, **, and *** represent statistical significance at 10%, 5%, and 1%, respectively.

Panel A: Excess Returns of Strategies				
Unmanaged Strategies	$CMKT$	EMI	WML	$EWML$
Excess Return	0.013**	0.025***	0.022***	0.034***
	(2.45)	(4.71)	(4.22)	(5.99)
Volatility-managed Strategies	$CMKT^{\sigma}$	EMI^{σ}	WML^{σ}	$EWML\ II^{\sigma}$
Excess Return	0.016***	0.023***	0.027***	0.035***
	(2.81)	(4.49)	(4.76)	(6.62)
Panel B: Univariate Regressions				
	(1)	(2)	(3)	(4)
	$CMKT^{\sigma}$	EMI^{σ}	WML^{σ}	$EWML^{\sigma}$
$CMKT$	0.957***			
	(31.63)			
EMI		0.941***		
		(15.05)		
WML			0.914***	
			(18.02)	
EWS				0.938***
				(19.42)
Alpha (α)	0.002	0.001	0.006***	0.001
	(1.28)	(0.47)	(2.62)	(0.48)
Adj R^2	0.901	0.846	0.826	0.844

Table A10. Robustness Checks on Different Ranking Periods and Holding Periods.

This table extends Table 4 to different ranking periods and different holding periods. Following Jegadeesh and Titman (1993), at each given week *t*, the strategies hold a series of portfolios selected at the current week as well as at the previous *K*-1 weeks, where *K* denotes the holding periods. Each week, the strategy holds *K* Elastic-minus-Inelastic long-short portfolios. Then we revise the weights on 1/*K* of these portfolios to get the average strategy returns. The excess returns, the Crypto-CAPM adjusted returns, the Crypto-three-factor model adjusted returns, and the Crypto-five-factor model adjusted returns of the long-short strategy are shown in this table. *T*-statistics adjusted by Newey-West heteroskedasticity with 5 lags are in parentheses. *, **, and *** denote statistical significance at 10%, 5%, and 1%, respectively.

	Ranking period	Holding Period				
		2	4	6	8	10
Excess Return	8	0.018***	0.021***	0.019***	0.028***	0.037**
		(3.33)	(3.70)	(3.49)	(3.90)	(2.55)
	10	0.025***	0.019***	0.019***	0.024***	0.024***
		(3.49)	(3.05)	(3.22)	(4.56)	(4.22)
	12	0.022***	0.019***	0.021***	0.023***	0.026***
		(3.81)	(3.17)	(3.29)	(4.35)	(3.79)
	14	0.016***	0.017***	0.020***	0.022***	0.021***
		(2.79)	(2.87)	(3.20)	(4.05)	(3.47)
	16	0.020***	0.016***	0.018***	0.022***	0.026***
		(3.02)	(2.69)	(2.90)	(3.98)	(3.54)
CAPM Alpha	8	0.020***	0.023***	0.021***	0.029***	0.022***
		(4.04)	(4.34)	(4.05)	(4.57)	(2.80)
	10	0.026***	0.021***	0.021***	0.026***	0.025***
		(4.17)	(3.67)	(3.71)	(5.14)	(4.72)
	12	0.025***	0.022***	0.023***	0.026***	0.027***
		(4.58)	(3.97)	(3.95)	(5.21)	(4.65)
	14	0.019***	0.019***	0.022***	0.025***	0.023***
		(3.62)	(3.56)	(3.82)	(4.92)	(4.16)
	16	0.022***	0.019***	0.020***	0.024***	0.027***
		(3.77)	(3.45)	(3.53)	(4.67)	(4.27)
Three factor	8	0.019***	0.021***	0.019***	0.028***	0.022***
		(3.80)	(4.15)	(3.84)	(3.82)	(2.80)
	10	0.026***	0.020***	0.020***	0.025***	0.023***
		(3.72)	(3.68)	(3.83)	(5.08)	(4.73)
	12	0.025***	0.021***	0.023***	0.025***	0.027***
		(4.80)	(4.13)	(4.05)	(5.40)	(4.37)
	14	0.018***	0.018***	0.020***	0.022***	0.021***
		(3.60)	(3.61)	(3.60)	(4.71)	(4.03)
	16	0.022***	0.017***	0.019***	0.022***	0.027***
		(3.37)	(3.39)	(3.44)	(4.54)	(3.81)
Five factor	8	0.018***	0.019***	0.019***	0.021***	0.042**
		(3.64)	(3.64)	(3.43)	(3.69)	(2.46)
	10	0.020***	0.019***	0.020***	0.023***	0.025***
		(3.32)	(3.43)	(3.66)	(4.19)	(4.28)
	12	0.024***	0.020***	0.021***	0.024***	0.024***
		(4.54)	(3.90)	(3.79)	(4.92)	(4.04)
	14	0.018***	0.019***	0.022***	0.022***	0.024***
		(3.60)	(3.82)	(3.65)	(4.35)	(4.42)
	16	0.014**	0.016***	0.017***	0.021***	0.022***
		(2.55)	(3.01)	(2.98)	(3.88)	(3.41)

Table A11. Predicting Cumulative Crypto Returns by Inelasticity

This table investigates the predictability of Inelasticity on cumulative returns using Fama-MacBeth regressions with different holding periods h:

$$Cumulative\ Ret_{i,t\ to\ t+h-1} = \alpha_t + \beta \times Inelasticity\ Dummy_{i,t-1} + \gamma \times X_{i,t-1} + \epsilon_{i,t},$$

where Inelasticity Dummy equals one if the cryptocurrency belongs to the highest quintile (i.e., top 20%) of Inelasticity. Control variables include Ret [a, b] (cumulative returns from the start of week $t+a$ to the end of week $t+b$), Size (logarithm of market value at the beginning of week t), lnAmihud (logarithm of average past 12-week Amihud illiquidity ratios prior to week t), Turnover (average past 12-week turnover ratios prior to week t), IVOL (idiosyncratic volatility based on Crypto-CAPM in the past 12 weeks prior to week t), Skewness and Kurtosis. We also control BA growth (the weekly growth rate of total addresses with balance at week t-1) and value (the negative of past-52-week return prior to week t) in columns (4) and (8). These two regressions begin in August, 2017 due to a limited cross-sectional sample size at the beginning of the dataset (less than 30 observations). The cumulative returns are winsorized at 1% and 99% percentiles. The bottom rows present the time-series averaged adjusted R^2, sample periods, and observations. Columns (1) to (4) present the results on 4-week holding periods and columns (5) to (8) report the results on 8-week holding periods. T-statistics adjusted by Newey-West heteroskedasticity with 5 lags are in parentheses. *, **, and *** denote significance at the 10%, 5%, and 1% level, respectively.

	(1)	(2)	(3)	(4)	(5)	(6)	(7)	(8)
Dep. Var =	Four-week Cumulative Ret				Eight-week Cumulative Ret			
Inelasticity Dummy	-0.062***	-0.048***	-0.050***	-0.052***	-0.100***	-0.076***	-0.076***	-0.044***
	(-6.46)	(-4.61)	(-4.73)	(-3.89)	(-7.09)	(-5.31)	(-5.31)	(-3.01)
Ret [-2, -1]		0.017	0.024	-0.061*		0.016	0.025	-0.035
		(0.99)	(1.25)	(-1.79)		(0.88)	(1.30)	(-1.36)
Size		-0.004	-0.004	0.002		-0.003	-0.003	-0.001
		(-0.87)	(-0.82)	(0.32)		(-0.35)	(-0.31)	(-0.11)
lnAmihud		-0.004	-0.004	0.007		-0.006	-0.004	0.008
		(-1.45)	(-1.02)	(1.07)		(-1.18)	(-0.54)	(1.15)
Turnover		-0.31	-0.006	0.068		-0.065	0.875	0.154
		(-0.84)	(-0.01)	(0.46)		(-0.10)	(0.85)	(0.86)
Ret [-12,-3]			-0.005	-0.008			-0.01	0.001
			(-0.58)	(-0.58)			(-0.85)	(0.07)
IVOL			-0.026	-0.046			-0.07	-0.025
			(-0.18)	(-0.22)			(-0.28)	(-0.11)
Skewness			0.015	0.009			0.01	0.007
			(1.47)	(0.88)			(0.59)	(0.41)
Kurtosis			-0.001	0.003			-0.001	0.002
			(-0.59)	(0.67)			(-0.32)	(0.43)
BA growth				0.149				0.108
				(1.26)				(0.51)
Value				0.004				0.009
				(0.77)				(1.15)
Adj R^2	0.010	0.035	0.051	0.064	0.009	0.023	0.038	0.061
Weeks	537	537	537	350	533	533	533	346
obs	383,168	383,166	383,161	94,478	376,756	376,754	376,749	93,014

Figure IN1. Dynamic Treatment Effect

This figure illustrates the dynamic treatment effects on Time (Panel A), AbVolume (Panel B), and Google Search (Panel C) during the [-3 weeks, +4 weeks] window around events. The figures display the coefficients associated with a 90% confidence interval of the dynamic treatment effect with controls.

Panel A: *Average Time Between Transactions*

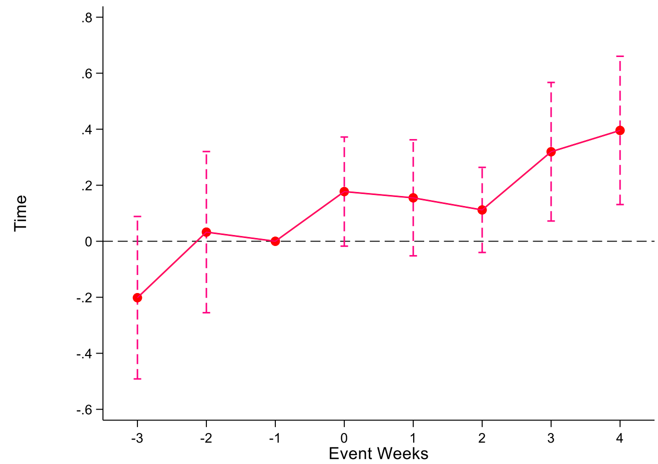

Panel B: *Abnormal Transactions*

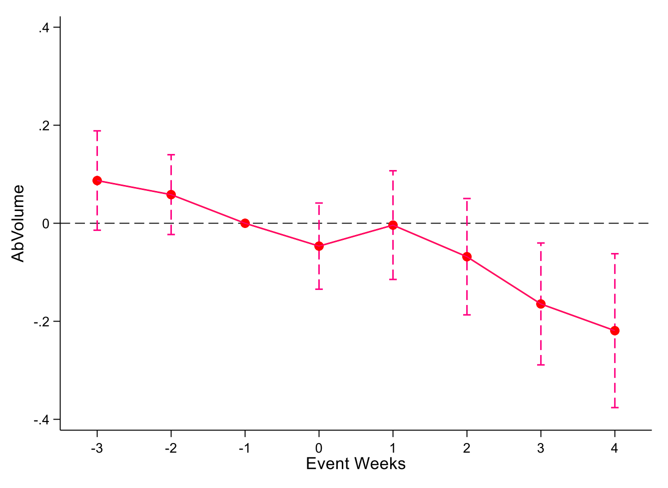

Panel C: *Google Search*

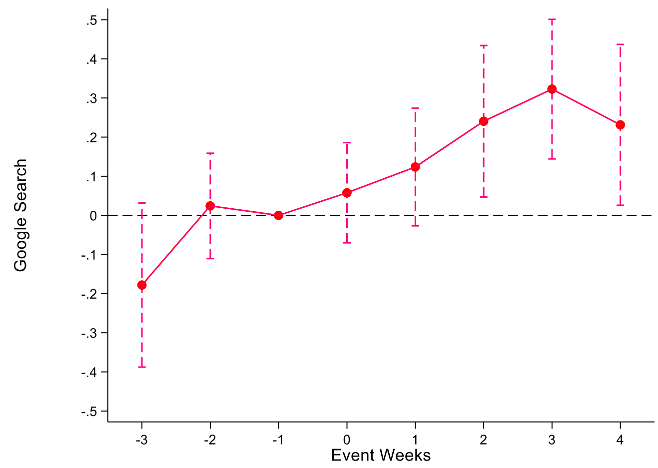

Figure IN2. Returns of EMI in Different Ranking Periods

This figure presents the single-sort Crypto-three-factor model alphas and Crypto-five-factor model alphas of the EMI (Elastic-minus-Inelastic) strategy based on InRanks and their 99% confidence intervals with different ranking periods (8-10-12-14-16 weeks). At the end of each week *t*-1, we split the cryptocurrencies into five quintiles based on their InRanks and hold the portfolios for one week. EMI strategy is constructed as the spread of value-weighted cryptocurrencies' returns between the lowest quintile (Elastic) and the highest quintile (Inelastic). Confidence intervals are based on Newey-West heteroskedasticity adjusted standard errors with 5 lags.

Panel A: *Crypto-three-factor model alphas of EMI strategy with different ranking periods.*

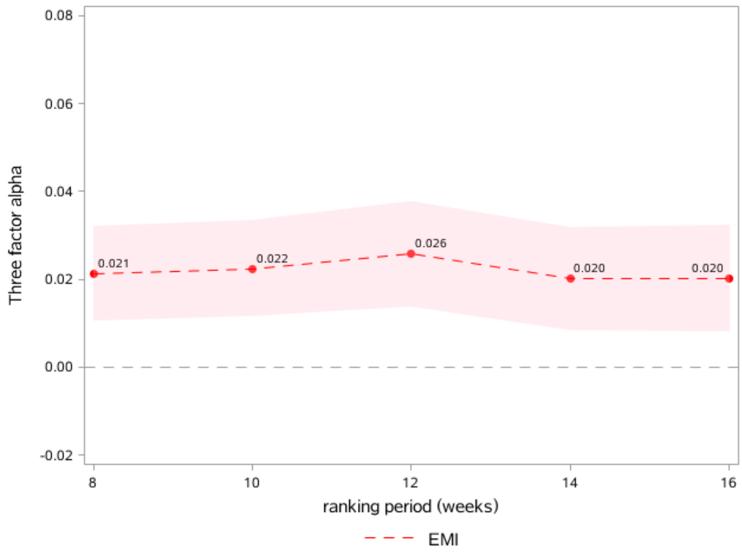

Panel B: *Crypto-five-factor model alphas of EMI strategy with different ranking periods*